

RL-83-024

COPY 1

Science and Engineering Research Council

Rutherford Appleton Laboratory

CHILTON, DIDCOT, OXON, OX11 0QX

SPAC, LASER

FILED IN STACK ROOM

LIBRARY
RUTHERFORD
18 JUL 1983
LABORATORY

Design Optimisation Studies for the GIOTTO Spacecraft Front Shield using Pulsed Laser Energy to Initiate a Flexural Wave Motion

D H Reading and A Ridgeley

May 1983

RL-83-024

© Science and Engineering
Research Council 1983

The Science and Engineering Research Council does not
accept any responsibility for loss or damage arising from
the use of information contained in any of its reports or
in any communication about its tests or investigations.

DESIGN OPTIMISATION STUDIES FOR THE
GIOTTO SPACECRAFT FRONT SHIELD
USING PULSED LASER ENERGY TO INITIATE A FLEXURAL WAVE MOTION

D. H. Reading
A. Ridgeley

A B S T R A C T

It is demonstrated that a pulsed laser beam can be used as a convenient and reproducible way to initiate a flexural wave motion in an aluminium sheet. This method was used to simulate the impacts of low mass, high velocity particles on the front shield of the Giotto spacecraft for the mission to Halley's comet. The design parameters of the front shield were studied using this technique in order to optimise the performance of the dust impact detection experiment (DIDSY) mounted on the front shield. A considerable improvement in experimental capability has been achieved as a result of these studies.

C O N T E N T S

	PAGE
INTRODUCTION	1
1. DESCRIPTION OF THE STIMULATING AND DETECTING SYSTEMS	
i. The Space and Astrophysics Division Laser	2
ii. The Sensors	3
2. THE BEHAVIOUR OF INDUCED BENDING WAVES ON AN ALUMINIUM SHEET	
i. Summary of the Theory of the Propagation of Waves	3
ii. Observation of the Direct Signal	4
iii. Observation of the Reflected Signal	5
iv. Observed Amplitude as a Function of Impact to Sensor Distance	5
v. Reproducibility of Observed Signals	6
3. TESTS WITH MODELS OF THE SPACECRAFT FRONT SHIELD	
i. Half Scale Model Showing Slowly Attenuating Travelling Waves	6
ii. Initial Tests to Introduce Damping	7
iii. Tests on a Full Scale Model, with Three Equal Sectors	8
iv. Tests on a Full Scale Model, with a 35° Sector	9
4. TESTS TO OBTAIN OPTIMAL JOINTS BETWEEN SECTORS ON THE FRONT SHIELD	
i. General Considerations - Theory	9
ii. A Set of Tests to Find Isolating Materials	11
iii. Tests to Simultaneously Measure Transmission and Reflection	12
a. The experimental arrangement	12
b. Reproducibility of observed signals	12
c. Results with single materials - riveted, brass or nylon screws	13

	PAGE
d. Results with combinations of materials	13
e. Factors other than isolating material that affect transmission	14
f. Joints that transmit well	16
iv. Tests to Minimise Coupling Through the Stiffening Ring	17
5. CONCLUSIONS	17
6. ACKNOWLEDGEMENTS	18
7. REFERENCES	20
8. TABLES	21
9. FIGURES	26
10. APPENDIX - "Propagation of flexural waves in plates" extract from internal report DIDSY/MKW/10(82) by M Wallis.	

INTRODUCTION

The work described in this report was in support of the Dust Impact Detection System (DIDSY), an experiment on board the GIOTTO spacecraft which is planned to pass by Halley's comet in March 1986. The GIOTTO mission is a project of the European Space Agency (ESA), and is described by Reinhard⁽¹⁾.

DIDSY is an experiment led by the University of Kent and involving several other groups including RAL. It is described by McDonnell et al⁽²⁾. The dust particles are detected by five systems mounted on a dual shield whose primary task is to protect the spacecraft during the 68 km s^{-1} encounter with the comet. The dual shield comprises a 1 mm thick aluminium alloy front shield and a thicker rear shield 250 mm behind the front shield. Particles large enough to penetrate the front shield generate a diverging cloud of debris which will impact the rear shield over a large area with much reduced penetrating ability.

Such large particles (10^{-3} - 10^{-6} g) are detected by a piezo-electric sensor mounted on the rear shield. Particles in the range 10^{-6} - 10^{-10} g are detected by three sensors on the front shield. The range 10^{-11} - 10^{-14} g is detected by differentially shielded penetration discharge capacitors, and masses 10^{-11} - 10^{-17} g are detected by an impact plasma sensor which also carries a piezo-electric sensor for the range 10^{-9} - 10^{-13} g.

The studies reported in this work are in support of the detection of the 10^{-6} - 10^{-10} g particles which will be detected by the three piezo-electric sensors mounted on the front shield. These studies involve the investigation of the design parameters of the front shield in order to obtain an optimum shield design for the DIDSY experiment subject to the limitations imposed by the structural requirements of the spacecraft.

In order to make these studies it was necessary to have some means of simulating the effect of high velocity microparticle impacts on the front shield. An ideal evaluation procedure would use a controlled laboratory source of 68 km s^{-1} projectiles of mass 10^{-6} - 10^{-10} g. Unfortunately, techniques do not exist to accelerate this particle mass range to that velocity. Electrostatic

dust particle accelerators can achieve such velocities only with lighter particles, and light gas guns can accelerate to velocities up to $\sim 10 \text{ km s}^{-1}$.

McDonnell⁽³⁾ has conducted experiments using glass beads of mass $\sim 10^{-4} \text{ g}$ at velocities $\sim 1 \text{ m s}^{-1}$, and with iron microparticles of mass $\sim 10^{-11} \text{ g}$ at velocities $\sim 6 \text{ km s}^{-1}$. He discusses the importance of small impact times and area and also the enhancement of momentum transfer due to large ejecta mass.

For the work described it was only necessary to generate signals similar to those which will be encountered, no absolute calibrations are included. In order to have an impact duration comparable to the mission impacts (ie $\sim 10^{-8} \text{ s}$), which is short compared with the relaxation processes, a laser pulse was used.

Although the laser beam has negligible momentum compared with a dust particle of similar energy it is known to impart a significant momentum impulse by ablative reaction of the hot plasma generated by the laser impact on the target. This method of simulating microparticle impact has been discussed by Burton⁽⁴⁾.

Measurements by Arad et al⁽⁵⁾ show a momentum impulse of $\sim 10^{-5} \text{ N s}$ is transferred by a 1J laser pulse at a power density $\sim 10^{14} \text{ W cm}^{-2}$. This is consistent with preliminary results using a ballistic balance at this laboratory which will be the subject of a later report. 10^{-5} N s is the momentum of a $\sim 10^{-7} \text{ g}$ particle at 68 km s^{-1} , and allowing for ablation, is the momentum transfer expected from a 10^{-8} - 10^{-9} g particle.

The Space and Astrophysics (S & AD) laser has an energy output of up to 20J in a timescale of up to 30 nanoseconds and can therefore impart momentum impulses which lie within the detection range of the DIDSY particle sensors on the front shield. The propagation tests to be described used this laser to simulate particle impacts.

1. DESCRIPTION OF THE STIMULATING AND DETECTING SYSTEMS

i. The Space and Astrophysics Division Laser

The laser as used consists of an oscillator and two amplifiers. The oscillator is a Q-switched neodymium glass device with a 30 ns FWHM pulse width

supplied by J-K Lasers Ltd. The amplifiers are custom-built neodymium glass rod amplifiers which give an output of 60 NW in a beam 16 mm in diameter. This system gave 1J on the target as measured with a calorimeter. The shot-to-shot variability in the laser energy was $\pm 7\%$. A spot size $\sim 300 \mu\text{m}$ was achieved by having the target about 3 mm closer to the 200 mm focal length lens than the focal point. This kept the focused power density below $10^{11} \text{ W cm}^{-2}$ thus allowing the experiments to be performed in air without the energy being dissipated by ionizing the air close to the target. A photograph of the laser system is shown in fig. 1. The optical set-up is shown schematically in fig. 2.

ii. The Sensors

The sensors used to detect the laser impacts were Dunegan/Endevco piezo-electric transducers type S1000BM described by Ching Feng and R M Whittier⁽⁶⁾. These sensors are the nearest commercially available type to the sensors to be used on the GIOTTO spacecraft. They were fixed to the underside of the propagating medium by means of a pressure pad and two fixing screws. No coupling material was used between the piezo-electric pad and aluminium plate. The spacecraft sensors will be fitted similarly except that they will have an integral mechanical clamp. These DIDSY sensors are optimised for a frequency in the region of 200 kHz, a frequency well above any expected spacecraft resonances which could produce spurious signals. A 200 kHz filter with $\pm 10 \text{ kHz}$ bandpass (to 3 dB) will be used in conjunction with the piezo-electric sensors to further restrict unwanted noise. The S1000BM sensors have a natural frequency of 300 kHz; however they were used with a 200 kHz filter for these tests to simulate the flight system. The output from the filters was fed directly into an oscilloscope or through a head amplifier (x 50 voltage).

2. THE BEHAVIOUR OF INDUCED FLEXURAL WAVES IN AN ALUMINIUM SHEET

i. Summary of the Theory of the Propagation of Waves

There are three kinds of elastic wave which can be propagated through a solid. The longitudinal or compressional wave is caused by displacements in the

direction of propagation, and the two shear waves by displacements transverse to the direction of propagation. Flexural or bending waves are a special case approximating to shear waves in which sheet material, thin compared with a wavelength, is displaced bodily in a direction transverse to the direction of propagation and the plane of the sheet. McDonnell⁽³⁾ has shown that stresses induced in sheet material by particle impact are coupled to piezo-electric sensors predominately by flexural waves. This was determined by observing their dispersive properties and the variation of velocity as a function of sheet thickness. In the experiments described in this report this identification is confirmed.

According to the Mindlin theory⁽⁷⁾ the respective group velocities for the longitudinal, shear and flexural motions are 5.4, 3.0 and 2.3 km s^{-1} in a 1 mm thick aluminium sheet at 200 kHz, and the wavelength of the flexural wave is 6.5 mm as the phase velocity is approximately half the group velocity. The application of this theory to the DIDSY experiment is summarised in the note by M Wallis appended to this report.

Aluminium is a low attenuation medium for flexural waves⁽⁸⁾, the internal dissipation arising from heat flow in the deformed material and from wave scattering at grain boundaries. In the absence of external damping the waves are able to travel distances of the order of 10^4 metres without appreciable attenuation.

ii. Observation of the Direct Signal

In a plate of finite size reflections from the edges give rise to complications in the response of the sensor. If the plate is sufficiently large that the reflections reach the sensor appreciably later than the direct signal then the response of a sensor mounted on an infinite plate can be simulated. Such an event is recorded in fig. 3 where a sensor was mounted near the centre of a 750 mm square plate and a laser impact made 200 mm from the sensor. The oscilloscope is triggered in synchronism with the laser pulse and the sensor response is seen to occur some time later. Fig. 3(a) shows the response without

a 200 kHz filter and fig. 3(b) the response with a 200 kHz filter which shows a pulse of duration 25 μs FWHM modulated at 200 kHz. By measuring the time of arrival of the pulse peak at different laser impact-sensor distances the group velocity is measured as 2.5 km s^{-1} . There is also a weak pre-pulse at a time corresponding to a group velocity about 5.5 km s^{-1} and this is attributed to the longitudinal vibration. This pre-pulse is more apparent when the 200 kHz filter is not in the system. The shear wave is apparently seen as a shoulder on the leading edge of the flexural wave pulse, corresponding to a velocity of 3.4 km s^{-1} . These velocities are in reasonable agreement with the theoretical values discussed in 2.i. A group velocity of 2.5 km s^{-1} for the flexural wave indicates a wavelength of 7.3 mm.

iii. Observations of Reflected Signals

An example of propagation including reflections is given in fig. 4. The configuration of the sensors and laser impact point is shown in fig. 4(a). Also shown in fig. 4(a) are the principal paths whereby a flexural wave can reach the sensors in the timescale of the oscilloscope trace. The oscilloscope trace is shown in fig. 4(b) and pulses corresponding to the time intervals depicted in fig. 4(a) can be clearly seen. The pre-pulses for both sensors are also clearly visible in this case as a less efficient filter was in use.

iv. Observed Amplitude as a Function of Impact to Sensor Distance

A sensor was mounted at the centre of a 1 m square plate and laser impacts were made at distances varying between 150 mm from the sensor to directly over the sensor. Fig. 5 shows a plot of sensor response against $1/\sqrt{r}$ where r is the distance from the sensor of the laser impact. The linear fit shows a good agreement with a $1/\sqrt{r}$ dependence which breaks down only at distances less or equal to the radius of the sensing pad on the sensor.

This $1/\sqrt{r}$ amplitude dependence is to be expected in a non-absorbing medium for a regime where dispersive processes have not lengthened the flexural wave train significantly. The wave train is in fact observed to be essentially unlengthened over this sort of distance.

Over greater distances dispersive processes would be expected to lengthen the pulse and a $1/r$ dependence might be found.

v. Reproducibility of Observed Signals

The experiments described in the preceding paragraphs are very reproducible both in amplitude and in pattern. The amplitude of the flexural wave motion is reproducible to 4%. This reproducibility removed the need to monitor any shot-to-shot variation.

In an experiment like that demonstrated in fig. 4 the exact pattern of the trace is repeated shot after shot provided the impact point and sensor locations are not changed and provided the sensor is not removed from the plate between shots.

3. TESTS WITH MODELS OF THE SPACECRAFT FRONT SHIELD

i. Half-Scale Model Showing Slowly Attenuating Travelling Waves

Initial tests were performed on an aluminium annulus 1 mm thick, 1 m outer diameter and 0.5 m inner diameter; a half-scale simplified model of the GIOTTO front shield. With a laser impact close to a single sensor a sequence of strong pulses was observed with a 900 μ s interval between them. This was attributed to the flexural wave travelling round and round the annulus with a period of 900 μ s per revolution. Between the strong pulses there were a mass of smaller pulses attributed to flexural wave motions propagating in random directions on the annulus. After the first pulses the amplitude sequence was found to be 7.5 : 6.5 : 5 : 4 indicating a time of some 35 ms to decay to 10^{-3} of the initial level. This amplitude sequence illustrates that aluminium is a low damping material and that reflections at the edges produce very little attenuation. In order to follow the wave propagation in greater detail two sensors were placed 120° apart on the annulus as shown in fig. 6a and laser impacts were made in locations (1), (2) and (3) shown in the diagram. The oscilloscope traces obtained are shown in fig. 6(b). The pattern of strong pulses obtained in the sensors can be seen to be very consistent with a flexural wave travelling in both directions around the plate with a period of 900 μ s.

When the 200 kHz filter was removed the overall signal increased by a factor 20 but the strong pulses were no longer clearly distinguishable above the random background.

The implications of this for the DIDSY experiment if mounted on an unbroken annulus is that there would have to be a long dead-time (~ 50 ms) following an event, causing saturation of the counting channels at an early stage in the comet encounter.

Advantage was taken of a decision by ESA to split the front shield into two sections for ease of integration to the spacecraft, by considering the possibility of inserting a damping material in the riveted joints. A search was therefore initiated to find a space qualified material which would damp the flexural wave if inserted in the joints.

ii. Initial Tests to Introduce Damping

Two aluminium plates, one 650 x 300 mm² the other 300 x 300 mm², were riveted together along one 300 mm edge by means of an aluminium connecting piece 30 mm wide. Candidate damping materials were inserted between the connecting piece and the aluminium plates as depicted in fig. 7(b). A sensor was mounted on each of the two plates. The laser was focused onto the larger plate in order to measure how much flexural wave energy was transferred to the smaller plate.

Initially three such experimental assemblies were made up. One with no damping material between the connecting piece and the plates, the others employing 1 mm thick silicone rubber in one case and 1 mm viton rubber in the other case. Little damping was observed for the straightforward aluminium riveted joint nor for the silicone rubber joint, but a considerable attenuation in the bending wave energy was noted for transmission across the viton joint.

In a further experiment a 250 mm square plate of aluminium was damped by riveting around the perimeter a 15 mm wide rim consisting of 1 mm thick viton rubber with 1 mm of aluminium to complete the sandwich. A sensor was mounted in the middle of the plate and the ringing time was measured after a laser impact. It was found that the ringing decayed by two orders of magnitude in about 300 μ s

compared with 5 ms for a similar plate without damping. It was concluded that viton rubber is a good damping material and experiments proceeded on the provisional assumption that viton would be used as a damping material in the spacecraft.

iii. Test on a Full Scale Model with Three Equal Sections

The GIOTTO bumper shield is essentially an aluminium annulus 1 mm thick with an outer diameter 2 m and an inner diameter 1 m. The annulus is fitted around the exhaust of the rocket motor by pillars attached to isolating pads on the inner edge, and to an aluminium stiffening ring 63 mm from the outer edge.

Following the ESTEC decision to split the front shield it was proposed that the shield be split into three 120° sectors with viton damping in each of the three joints. A sensor would be mounted in each joint on a bridge joining the two adjacent sectors 60 mm inboard of the stiffening ring centre line. This arrangement was simulated by building a full-size model in the laboratory for testing. A photograph of the model is shown in fig. 8(a) and the schematic arrangement is shown in fig. 8(b).

Laser impacts were made at various points on this mock-up shield to test the efficiency of the isolating joints and to determine the radial and azimuthal variation of response of the sensors as different parts of a segment were impacted. Pulse height variation at distances greater than 200 mm from the detectors was found to be about 3:2 in both azimuthal and radial directions. By comparing laser pulses impacting on either side of a joint it was possible to estimate the transmission of a joint to be about 5%. With viton damping in the joints the time for decay to 10^{-3} in amplitude was approximately 5 ms.

By adding extra damping at either the inner edge or near to the outer edge the time constant could be reduced to 2-3 ms but at the expense of greater variability of response over a segment.

The effect of drilling the two holes A and B (50 mm and 75 mm diameter respectively), representative of holes which would actually be present in the spacecraft shield, was investigated. The presence of the holes in fact had

surprisingly little effect. The presence of hole A produced no significant change in signal at sensor 1, even when the laser was fired close to the hole in position (i). The effect of hole B was to increase the signal at sensor 1 by 50% with the laser fired at position (ii) and to decrease it by a factor 2 with the laser fired at position (iii).

iv. Tests on a Full Scale Model with a 35° Sector

The above tests proved the viability of a three-sector shield with isolating joints. At this stage, however, it was considered that a further improvement in experimental performance would be obtained if the three-sector shield was made with one transmitting joint and with the two isolating joints about 35° apart so as to have two separate shield areas a factor ten different in size. The small sector could then be free from holes and other discontinuities which would degrade the detection of dust particle impacts.

To evaluate this new design the shield was modified to incorporate such a 35° sector. In this arrangement a sensor was placed on the 35° sector on the centre line 40 mm from the inside edge with two more sensors on bridges between the 35° sector and the rest of the shield. The response of the 35° sector is shown in fig. 9 which also shows the laser impact positions selected for mapping the response. As can be seen from fig. 9 the overall variation in sensitivity is about 3:1 except close to the sensor. The decay time for 10^{-2} in amplitude was 2.5 ms.

4. TESTS TO OBTAIN OPTIMAL JOINTS BETWEEN SECTORS ON THE FRONT SHIELD

i. General Considerations - Theory

The type of joints investigated in this work for the most part employed the principle of constrained layer damping. A constrained layer of damping material consists of a composite laminate made up of a damping core material sandwiched between skins of structural material in a triple or multi layer. The damping action is a direct result of shearing of the viscoelastic core material as the laminate is flexed. This method of damping allows the structural integrity of

the composite to be preserved. A fuller account of layer damping is described by Cooney and Thorn⁽⁹⁾.

In order to estimate the effect of signals from the large sector swamping the small sector at high flux rates we have calculated the detection efficiency at 30 seconds from closest encounter, ie 2000 km from the core of the comet, assuming the dust distribution estimated by the Science Working Team in May 1981⁽¹⁰⁾. The electronics was assumed to generate a dead time after each signal in the form of a discriminator threshold which reduced exponentially at the same rate as the signal level. Any signal larger than the threshold would be accepted, false signals, eg from the other sector, being deconvoluted after data collection. It was found that with no coupling between sectors the efficiency of the electronics associated with the small sector was 40% for the 10^{-9} - 10^{-10} g mass bin and 90% for the 10^{-8} - 10^{-9} g mass bin. These efficiencies were found to be depressed to 33% and 86% respectively by a 0.1% cross-talk from the large sector and to 13% and 75% respectively by a 1% cross-talk. It is therefore very desirable, in order to make use of the enhanced capability of the shield, to reduce transmission across the joint to below 1% and if possible to 0.1%.

The remaining joint needs to be reasonably close to 100% transmitting in order for the two large plates to function as one sector. It was also necessary to investigate and, if necessary, eliminate any problem due to transmission through the outer stiffening ring. In order to accomplish these objectives it was necessary to carry out a systematic testing of joint materials in order to find the best way of optimising the joint construction.

The problem of constructing the isolating joint appeared to be the most important one so efforts were directed primarily towards determining the construction necessary for this joint. Since this joint also has to damp the reflected wave as well as isolate the small segment it had to conform to the following exacting requirements:

reflection from joint < 20%

transmission across joint < 0.1% if possible but in any case < 1%

ie. isolation across joint > 99.9% if possible but in any case > 99%

Initial tests concentrated on finding materials which when inserted in the joint would give a low transmission, although it was understood that some of these would accomplish this by means of high reflection.

ii. A Set of Tests to Find Isolating Materials

The experimental arrangement shown in fig. 10 was set up in which two aluminium plates were jointed together by means of an aluminium connecting piece screwed to both aluminium sheets with the candidate material sandwiched between the sheet and connecting piece as in fig. 7(b). Nylon screws were used as it was anticipated that they would not transmit the flexural wave readily along their length. A laser impact was located halfway between two sensors (one on each plate) and the ratio of the two signals gave the transmission of the joint. Variations in sensor sensitivity were allowed for by calibration laser shots on each plate.

Various materials were tested using this arrangement. Viton gave 7% transmission in this joint. Various materials gave lower transmission including, epoxy fibreglass sheet, PTFE, mica and layers of aluminium foil. Epoxy fibreglass gave the lowest transmission, 0.1% within ~ 100 μ s (prompt) and 0.7% (delayed) observed sometime later. In this and other cases where a larger delayed signal is observed, the timing of the delayed signal corresponds to reflections from the edges of the plates crossing the joints at oblique incidence. Silicone rubber gave the highest transmission (31%) this result being relevant to the design of the good transmitting joint. Results are given in Table A, and material specifications in Table E. A discussion on the level of confidence assignable to this and the following results may be found in 4.iii.b. below.

The effect of transmission through the nylon screws was investigated by a test in which there was negligible sandwich material, the connecting piece being

spaced off the plates by means of nylon washers 2 mm thick with outer diameter 10 mm and inner diameter 3.5 mm. This test gave a transmission of 0.6% (prompt) and 1.3% (delayed) indicating that no further isolation is to be expected for isolating as opposed to absorbing materials in this type of joint.

A double sandwich joint using viton plus fibreglass gave a transmission of 0.1% (prompt) and 0.2% (delayed) indicating that damping by the viton can reduce the transmission through the screws.

iii. Tests to Simultaneously Measure Transmission and Reflection at a Joint

a. The experimental arrangement. In order to measure reflectivities of joints as well as transmissions the larger experimental arrangement shown in fig. 11 was built. Sensor 1 was used as a monitor sensor, the ratio of the reflected pulse onto sensor 2 to the direct pulse onto sensor 1 giving the reflectivity. Likewise the ratio of sensor 3, response to sensor 1 response gives the transmission. The three sensors were calibrated relative to each other by means of laser impacts at a standard distance from each sensor. The distance of 300 mm for the wave to travel before reaching its appropriate sensor was chosen in order to resolve the initial pulse on sensor 2 from the reflected pulse onto sensor 2. The slot between the laser impact and sensor 2 was put in to reduce the size of the direct pulse on sensor 2 and thus to reduce its residual interfering effect on the reflected pulse to an estimated 5%. Direct measurement showed that the slot did not change the wave amplitude at launch or reception by more than 10%. The overall dimensions of the plates were chosen so as to resolve the measured pulses from later pulses reflected from the edges of the plates. As well as riveted joints, demountable joints using brass M3 nuts and bolts were used tightened to just below their shearing point (≈ 100 g cms) to simulate rivet pressure. Nylon nuts and bolts were also investigated. The simpler fig. 10 assembly was still used from time to time using brass screws or rivets.

b. Reproducibility of observed signals. The variation of measured reflectivity and transmission at joints among different but similar joints is greater than the

laser variability. An analysis of all measured variations shows that any given joint is only representative to $\pm 40\%$. The major cause of variability has not been isolated but joint pressure, joint distortion, sensor contact, interference effects and laser impact position have been found to have a strong influence on individual samples.

c. Results with single materials - riveted, brass or nylon screws. As a reference point assemblies as in fig. 11 were made up with viton rubber in a joint which was riveted together. This joint gave the following results:

reflected	15%
transmitted	$3.0 \pm 0.9\%$

Using nylon screws instead of rivets the reflectivity measured 55% with transmission of 7%. The high reflectivity was attributed to lack of pressure in the nylon screws and this was the reason for the change to brass screws. With brass screws the reflectivity was 30% with 3.4% (prompt) transmitted. The lowest transmitting materials tested with nylon screws on the small assembly were fibreglass laminate and PTFE. These materials were re-tested using brass screws in the large assembly. The transmission measurements were 2% and 4% respectively with reflectance measurements indistinguishable from 100%.

Also tested were Kevlar laminates and some resin-based elastomer materials, solithane and other polyurethanes at different hardness of mix. Kevlar is to be used on the rear shield and Solithane had been used as an acoustic damping material on IUE. All of these gave transmissions of a few percent with high reflectance. Kevlar gave 1.5% transmission with 100% reflectance. One polyurethane mix gave 13% transmission with 73% reflection indicating that 14% of the energy was absorbed. This was the only material apart from viton and silicone rubber in which any absorption was observed. With silicone rubber 15% was reflected with 31% transmitted. Results are tabulated in Table A and material specifications in Table E.

d. Results with combinations of materials. It being apparent that no single material was likely to be found that would achieve the necessary isolation plus

damping the next thing tried was combinations of two materials. It was decided that one of these had to be viton rubber because of its high attenuation. For simplicity the configuration chosen initially was that depicted in fig. 7(d) in which an isolating material is sandwiched along with viton in a simple riveted or bolted joint. Of the materials tested the best results were obtained with 1 mm epoxy Kevlar with 0.2% transmission. Phenolic Kevlar gave 0.6% transmission and melamine fibreglass gave 1% transmission with 10% reflection. None of these materials have been rated yet as space approved. 1.6 mm epoxy fibreglass gave 0.6% transmission when riveted, 0.8 mm gave 3.7%. 2 mm riveted space rated epoxy Kevlar yielded 1.0% transmission with 20% reflection. These results are tabulated in Table B and material specifications in Table E.

e. Factors other than isolating material that affect transmission. The factors studied and reported on below are rigidity of the joint; rivet pressure; rivet pitch and connecting piece rigidity and width; viton thickness; and temperature.

The residual transmission through this type of joint is largely attributed to the rigidity of the joint rather than the materials which comprise the joint. This view was obtained from the following tests which show that transmission correlates with joint rigidity.

- i. A joint as shown in fig. 7(b) with an epoxy fibreglass isolating layer bonded in place with epoxy resin and without using screws or rivets gave a transmission of 32%.
- ii. A brass screwed joint as shown in fig. 7(b) with a single epoxy fibreglass layer but with epoxy fibreglass shoulder washers to isolate the bolts from the metal sheet gave a transmission of 6%.
- iii. If the fibreglass isolating material is removed in joint (ii) and the aluminium spaced off with 1.8 mm thick PTFE washers 10 mm in diameter the transmission is still 6%.
- iv. The joint illustrated in fig. 7(i), in which the isolating part of the joint is separated from the attenuating part,

transmitted 1.8% which is no improvement over a joint in which these functions are not de-coupled.

- v. Joints made using nylon screws, which could not be tightened as much as metal screws or rivets, transmitted less than similar joints using brass screws or rivets. See also the pressure tests below.
- vi. Having shown that rigidity in a joint limits its isolating performance the joint shown in fig. 7(j) was produced. This joint differs from joint 7(i) in that the epoxy fibreglass material in the isolating joint is only 0.4 mm thick, and is bolted alternatively to one aluminium piece or the other. This joint, which was designed to have mechanical strength combined with flexibility, was found to transmit only 0.5%. With a 0.5 mm strip of viton bonded to the fibreglass strip using "Permabond 910" superglue the transmission dropped to below 0.05% which was the lower limit of measurement set by noise in the head amplifiers. Table C lists results from such complicated joints.

The effect of rivet pressure was investigated by making up an assembly like fig. 10 in which steel nuts and bolts were used in a joint incorporating 1 mm viton plus 0.8 mm epoxy fibreglass, and the transmission was measured as the bolts were gradually tightened from finger-tight to beyond that obtained with brass nuts and bolts or with rivets. The results are shown graphically in fig. 12. The curve demonstrates the conflicting effect of joint rigidity and compression of the viton. As the joint is tightened it becomes more rigid and transmits better. However, as the viton is compressed it attenuates better and eventually a point is reached where this effect dominates over the increasing rigidity.

A joint with viton plus 0.8 mm epoxy fibreglass was tested with 15 mm rivet pitch instead of 30 mm rivet pitch and was found to transmit 1.6% as opposed to

3.7%. Another joint with viton plus 1.6 mm epoxy fibreglass was made with a rivet pitch of 60 mm but with the rivets staggered on either side of the joint. This joint transmitted 0.4% and reflected 30%. Similar joints with the usual 30 mm rivet spacing transmitted about 0.6%. When the rigidity of the connecting piece of a similar 60 mm rivet pitch joint was increased, by having 1.5 mm lips on its edges and those of the sheets, the transmission increased to 1.2% and the reflection reduced to 20%. A standard 30 mm pitch joint with 1 mm viton only transmits 3% and reflects 15%. Reducing the rigidity, by chamfering 15 mm at the edges to a wedge, resulted in the transmission rising to 6% surprisingly and the reflection to 60%. Without chamfering, but with a 20 mm rather than the standard 30 mm wide connecting piece, the transmission rose to 5% and reflection to 36%.

Three thicknesses of viton were tested in a single layer joint, fig. 7(b), 0.5 mm, 1 mm and 2 x 1 mm. The transmissions were respectively 18%, 3% and 1.8%.

The dependence on temperature was tested on two viton and Kevlar (epoxy or phenolic) joints as in fig. 7(d) on sheets similar to fig. 10 which gave prompt transmission of 0.2% and 0.6% respectively at room temperature. On both cooling to -75° C and heating to 90° C the prompt transmission doubled. The delayed transmission while unaltered at 90° C increased by a factor ~ 6 for the epoxy Kevlar when cooled. The sensor sensitivity remained constant within a factor of two and although the reflectivity could not be measured the time taken for signals to decay to 1% stayed constant at ~ 7 ms. Individual measurements proved difficult to reproduce indicating that thermal history may play an important role.

f. Joints that transmit well. It was the discovery that the rigidity of a joint is increased by bonding it using epoxy resin which provided the means of optimising the third joint for good transmittance. Earlier measurements had shown that a joint in which the segments were directly riveted together by means of a 30 mm wide connecting piece transmitted only 22%. This transmission was increased to 70% if the joint was bonded together using epoxy resin as well as rivets. The measured reflection from this joint was 38%. When bonded with

silicone rubber as well as riveted a transmission of 17% (prompt), 39% (delayed) was obtained with 11% reflection.

A different way of joining the sectors, namely using a single 1 mm viton strip between a 15 mm perpendicular lip on each sector, produced a transmission of 28% and a 35% reflection. This type of joint was not studied further.

iv. Tests to Minimise Coupling Through the Stiffening Ring

The transmission via the stiffening ring was investigated using test rigs in which two plates were joined together by means of a simulated section of stiffening ring (fig. 13). A laser impact on the larger plate produced 4% transmission through the stiffening ring. The signal transmitted this way was observed at a later time than those previously transmitted through the main joint. The signal decayed with a time constant appropriate to the larger plate.

This transmission could not be reduced either by spacing off the small plate from the stiffening ring with washers or by having a continuous strip of viton or other material between the stiffening ring and the small plate.

The transmission could only be reduced to an acceptable level by breaking the stiffening ring between the plates and re-joining it using a connecting piece with viton damping, or by having a de-coupled strip (as in fig. 7(j)) between the stiffening ring and the small plate.

The former solution reduced the transmission to 0.15%, the latter to below the detection limit of 0.05% if the strip of fibreglass had a strip of 0.5 mm viton bonded to it using "Permabond 910" superglue. Results are tabulated in Table D and material specifications in Table E.

5. CONCLUSIONS

i. It has been confirmed that the energy in a pulsed laser beam can be used to impart momentum into a mechanical system and thus simulate high velocity dust particle impacts. In these studies this momentum was detected in the form of a flexural wave motion whose temporal and spatial development could be traced with piezo-electric sensors. The velocity and distance amplitude dependence agree with theoretical predictions.

ii. Various parameters which affect the wave propagation properties of the DIDSY front shield have been investigated using the laser impact technique, and the following ways of optimising performance found. Results are also tabulated in Tables A-D.

- a. Viton rubber is found to be a good attenuating material when used under compression in a layer joint. Joints incorporating viton typically reflected only 20% of the incident wave amplitude. This results in a reduction in decay time to 10^{-3} in amplitude from about 35 ms to about 5 ms for a 120° shield sector and to about 3.5 ms for a 35° sector.
- b. Isolation between the sectors is best achieved with a joint like 7(j) in which there is a flexible coupling between the sectors, joints like 7(d) can achieve better than 99% isolation however with a suitable isolating layer (eg. Kevlar laminate).
- c. A joint which is bonded for rigidity will transmit well (70%).
- d. The stiffening ring was found to be an important source of cross-talk between the small and large sectors. This problem can be solved either by having joints in the stiffening ring like 7(b) between the sectors, or by mounting the ring onto the small sector as in fig. 7(j).

6. ACKNOWLEDGEMENTS

The authors would like to thank and acknowledge the contributions made by the following people in the course of the work:

W M Burton and B C Fawcett who proposed using the momentum imparted by the recoil of a laser-produced plasma for measuring the propagation of flexural waves.

M K Wallis, University College Cardiff, for investigating the theoretical aspects of flexural wave propagation, and for permission to include part of his paper as an appendix in this report.

R W Hayes for setting up the laser optics and his assistance in demonstrating the initiation of bending wave motion using laser pulses.

E C Sawyer for providing the sensors and above all for coming forward with viton rubber as a possible damping material.

J Pateman and A Dean for their valuable workshop assistance,

D Evans and D Morrow of Chemical Technology for their assistance in preparing polyurethane mixes and in investigating bonding methods using epoxy resins, silicone rubber and superglue adhesives.

7. REFERENCES

- Reinhard, R., Space Missions to Halley's Comet and Related Activities. ESA Bulletin No 29, February 1982, p 68.
- McDonnell, J.A.M., Grün, E., Evans, G.C., Turner, R.F., Firth, J.G., Casey, W.C., Kuczera, H., Alexander, W.M., Clark, D.H., Grard, R.J.L., Hanner, M.S., Hughes, D.W., Igenbergs, E., Lindblad, B.A., Mandeville, J.C., Schehm, G. and Sekanina, Z. ESA SP-169 (1981).
- McDonnell, J.A.M., J. Sci. Instr. (J. Phys. E.) 2, p 1026 (1969).
- Burton, W.M., RL-82-030 (1982).
- Arad, B., Elieger, S., Jackel, S., Krumbein, A., Loebenstein, H. M., Halzmann, D., Zigler, A., Zinova, H., Zweigenbaum, S., Phys. Rev. Letts 44, P326 (1980).
- Ching Feng, Whittier, R. M., Acoustic Emission Transducer Calibration Using Transient Surface Waves and Signal Analysis. Dunegan/Endevco Technical Report No DE 79-1.
- Graff, K. F., "Wave Motion in Elastic Solids", Clarendon Press (1975).
- Mason, W. P., "Acoustic Properties of Solids", Am. Inst. Physics Handbook, Ch. 3f, 3rd ed. (1972).
- Cooney, J.P., Thorn, R.P., ASME Publication No 64-WA/RP-8 presented at the Winter Annual Meeting of the ASME, New York, 29 November-4 December (1964).
- Minutes of 2nd GIOTTO Science Working Team, April 1981, Appendix 4. Unpublished.

8. TABLES

TABLE A: SIMPLE JOINT (as on figure 7(b))

Material	Thickness (mm)	Fixing					Transmission %		Reflection %	Number of separate transmission tests
		screws (nylon)	screws (brass)	rivets	bonded	bonded & rivets	Prompt	Delayed		
None				✓		#	6	22	68	1
						±	70	>	38	1
							17	39	11	1
Viton	0.5			✓			18	>	71	1
	1 (x 10)			†			5	>	36	1
	1	✓					6±2	10±3	55	2
	1		✓				3.4±.6	6.5±3	30±5	3
	1			✓			3.0±.9	>	15	2
	1				*	#	4.5	>	12	1
	1						4.9	>	32	1
	1		X				6	>	60	1
	2 x 1		✓				1.8	2.9		1
PTFE	0.8		✓				2.7	22	~100	1
	2 x 0.8	✓					0.2	0.4	-	1
	2 x 0.8		✓				1.7	3.9	~100	1
Melamine/glass fibre laminate	0.8		✓			#	0.3	2.5	~100	1
	0.8						6.7	>	~100	1
	1.6		✓				0.6	2.8	~100	1
Epoxy/glass fibre laminate	1.6	✓					0.1	0.7	~100	1
	1.6		✓				0.5	2	~100	1
	1.6				#		32	>	39	1
Silicone rubber	1.0	✓					22	>	-	1
	1.0		✓				23	>	32	1
	1.0			✓			31	>	-	1
	1.0		±				51	>	26	1
	1.0			±			24	38	40	1
Sollithane	(hard) ~1		✓				3.6	7.5	~100	1
	(med.) ~1		✓				2.5	4.8	~100	1
Polyurethane	(cold cure)		✓				3.7	12.6	73	1
Epoxy/Wilsonite	~1		✓				1	3.3	~100	1
Kevlar (Epoxy)	2		✓				1.5	>	~100	1
Mica	2 x ~0.5	✓					0.4	1.2	-	1
Nylon washers	2	✓					0.5	1.3	-	1
Al	5 x 0.1	✓					1.5	3	-	1
Glass cloth	4 layers	✓					0.1	0.4	-	1

Bonded with epoxy resin

± Bonded with Silicone Rubber

* Bonded with "Permabond 910" superglue

† 20 mm wide joint rather than standard 30 mm.

X Chamfered edges

- No measurement made.

> Not significantly larger.

**TABLE B: DOUBLE SANDWICH (As in figure 7d)
ie. 1 mm viton plus test material**

Second Material	Thickness (mm)	Fixing			Transmission %		Reflection %	Number of separate Transmission Tests
		screws (nylon)	screws (brass)	rivets	Prompt	Delayed		
PTFE	2 x 0.8		✓		2.5±1.3	>	20±6	4
Epoxy	0.8		X		4.5	>	-	1
fibreglass	0.8			✓	3.7	>	-	1
laminate	0.8			†	1.6±.2	>	-	2
	1.6	✓			0.1	0.2	-	1
	1.6		✓		1.9±.3	2.8	18±4	2
	1.6			*	0.4	1.2	30	1
	1.6			✓	0.55	>	-	1
	1.6			‡	1.2	>	20	1
Melamine	0.8			✓	1.0±.2	>	7	2
fibreglass	1.6		✓		1.1	>	17	1
laminate	1.6			✓	1.0±.4	>	10±1	2
Epoxy Kevlar	1			✓	0.2±.1	0.3	-	2
" "	2		✓		0.3	0.9	-	1
" "	2			✓	1.0	>	20	1
Phenolic Kevlar	1			✓	0.6±.2	>	-	2
laminates								

X steel screws

† 15 mm apart instead of standard 30 mm

* 60 mm apart instead of standard 30 mm (rivets staggered 30 mm)

‡ As * but edges lipped.

> Not significantly larger

- No measurements taken.

TABLE C: VARIOUS JOINTS (As figure 7 except (b) and (d))

Material Other than 1 mm Viton	Thickness (mm)	Fixing	Transmission %		Reflection %	Number of Separate Transmission Tests
			Prompt	Delayed		
Just Viton		Fig 7a brass screws	10	>	-	1
PTFE		brass screws	3.7	>	12	1
Melamine fg	1.6	rivets	7.3	>	-	1
Epoxy fg	1.6	Fig 7c brass screws	2.1	>	-	1
Just Viton		Fig 7f brass screws	1.4	1.8	22	1
PTFE	2 x 0.8	Fig 7f brass screws	0.5 ± .2	1.1 ± .3	21 ± 2	2
PTFE	2 x 0.8	Fig 7e brass screws	0.8	>	22	1
Melamine fg	1.6	Fig 7e brass screws	3.5	>	12	1
Epoxy fg	1.6	Fig 7e nylon screws	< .01	0.3	-	1
PTFE	2 x 0.8	Fig 7g brass screws	0.7	0.9	40	1
PTFE	2 x 0.8	Fig 7h brass screws	1.2	>	15	1
PTFE + Viton	2 x 0.8 †	Fig 7h brass screws	2	3.3	20	1
Epoxy fg	1.6	Fig 7i brass screws	1.8	>	49‡	1
Epoxy	0.4	Fig 7j brass screws	0.5	>	32	1
Epoxy fg + bonded Viton	0.4 + 0.5	Fig 7j brass screws		< 0.05	17	1
Polyurethane	~ 1	Fig 7j brass screws		< 0.05	21	1
Al + bonded Viton	0.5 + 0.5	Fig 7j brass screws	0.33	0.5	37	1

fg fibreglass laminate

> Not significantly larger

† with extra 1 mm Viton directly above sector and beneath the PTFE

- No measurement made

‡ large reflection due to a distorted sector

TABLE D: STIFFENING RING TRANSMISSION TESTS

The prompt signal through the stiffening ring is very small. The signal rises to a maximum at $\sim 500 \mu s$, 75% of which is reached by $150 \mu s$. The signal falls after the maximum with a time constant determined by the large sector. Tests were conducted on the rig shown in Fig. 12. Radial dependance was found to be $\sim 2:3$. For the results quoted below the laser impact was at point 1 and the detector was at A. Only one sample of each method of fixing was used.

Method of Fixing the Stiffening Ring to the Sectors				Response at 500 μs (%)
Type of Fixing	Pitch (mm) on Small Sector (30 mm on Large)	Spacer Material		
		Thickness	Type	
Rivets	30	-	None	2
		1 mm	Viton washers	3
		1.6	Epoxy g.f. washers	3.5
Screws	30	1	Viton washers	3
	120	1	Viton washers	1.6
	120	1	Also under head and nut	1.7
	120	0.8	PTFE washers	1.4
	30	0.8	PTFE strip	1.6
	60	0.8	PTFE strip	1.3
	30	1	Viton strip	2.8
	120	1	Viton strip	2.1
	60	1	Viton strip	1.7
		+ 0.8	PTFE strip	
Screws holding spacer alter- nately to sector and ring	30	0.4	Kapton strip	.2
	30	0.5	Al strip	.9
	30	0.5	Al* strip	.2
	30	0.4	Epoxy g.f.* strip	<.04
	30	0.4	Kapton* strip	.08
	30	0.4	Kapton** strip	.07
Stiffening ring cut and joined with riveted Al strip with 1 mm Viton spacer	30	-	None	.15

g.f. Glass fibre laminate

* Material type marked * had 1 mm Viton strip bonded with "Permabond 910" superglue

** Material type marked ** had 0.5 mm Viton strip bonded with "Permabond 910" superglue

TABLE E: MATERIAL SPECIFICATIONS

Quoted Material	Technical Specification (Where Known)
Viton Rubber	Shore Hardness 75
Silicone Rubber	-
PTFE	BS 3784 Type 1
Epoxy Fibreglass	BS 5953 EP(1) and EP(2)
Melamine Fibreglass	BS 5953 MF(1) and MF(2)
Epoxy Kevlar	Fiberite MXM 7714A
Phenolic Kevlar	Hexol R1610-49-120U
Space-rated Kevlar	Hexol F155-49-281
Solithane (Thiokol Chemicals Ltd)	Type 113 Recipe #1 (hard) #4 (medium)
Polyurethane (Baxenda Chemicals Ltd)	ES700 Ratio 4:1
Glass Cloth	-
Mica	Ruby Mineralogical Group Muscovite
Kapton	-
Wilsmite (CIBA Geigy)	XD 760

9. LIST OF FIGURES

1. Photograph of Laser.
2. Schematic Arrangement of Laser Optics.
3. Oscilloscope Traces of Flexural Wave Pulse.
- 4(a). Schematic of Experimental Arrangement Illustrating Edge Reflections and Observed Transit Times.
- 4(b). Oscilloscope Traces Obtained from Experimental Arrangement Shown in figure 4(b).
5. Graph Showing $\sqrt{1/r}$ Dependence of Sensor Response.
- 6(a). Two-sensor Arrangement on Half-scale Annulus.
- 6(b). Oscilloscope Traces Obtained from Experimental Arrangement Shown in figure 6(a).
7. Various Sector Joints.
- 8(a). Photograph of DIDSY Shield Mock-up.
- 8(b). Schematic Arrangement of Full-sized Model of DIDSY Bumper Shield.
9. Measured Response Over 35° Sector.
10. Schematic Diagram Showing Experimental Arrangement Used to Measure Transmission of Joints.
11. Experimental Arrangement to Measure Reflectivity as well as Transmission of Joints.
12. Effect of Bolt Pressure on Transmission.
13. Experimental Arrangement to Study Effects of Stiffening Ring.

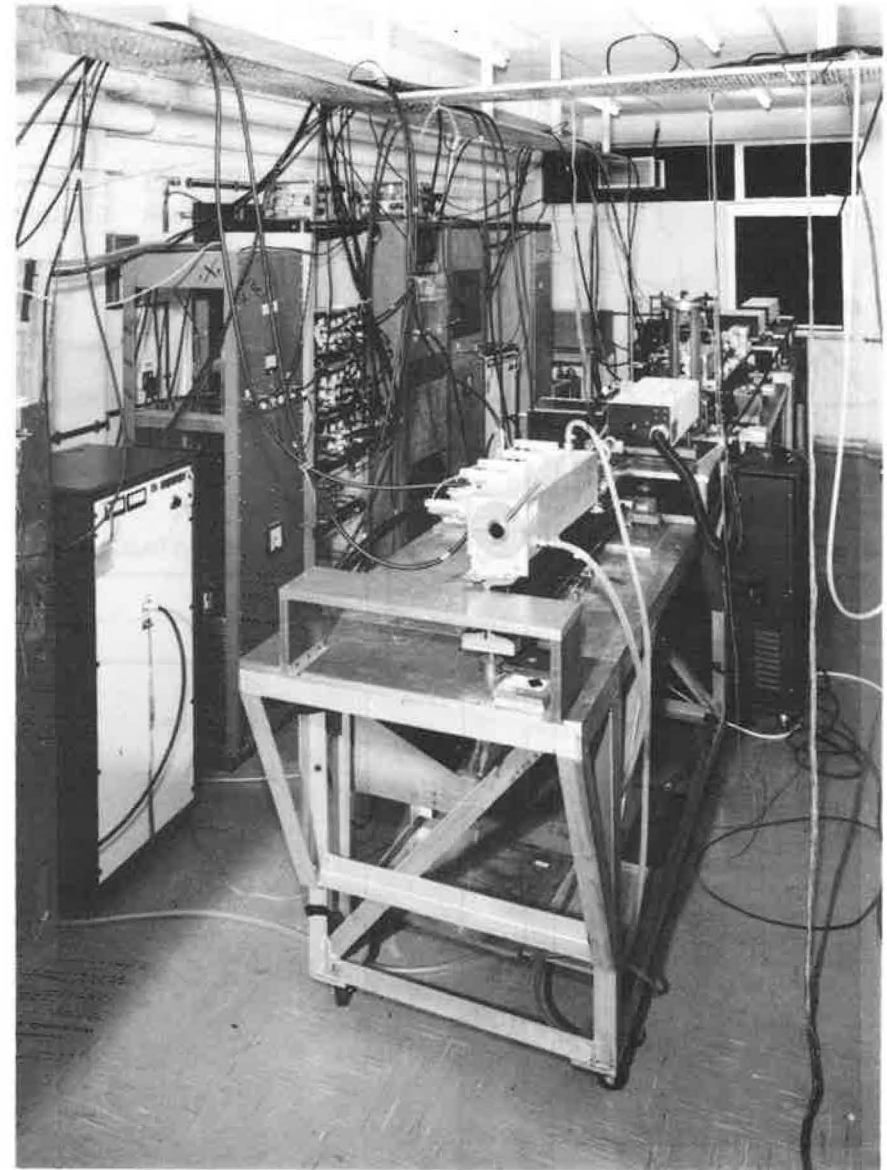


Fig.1 Photograph of Laser

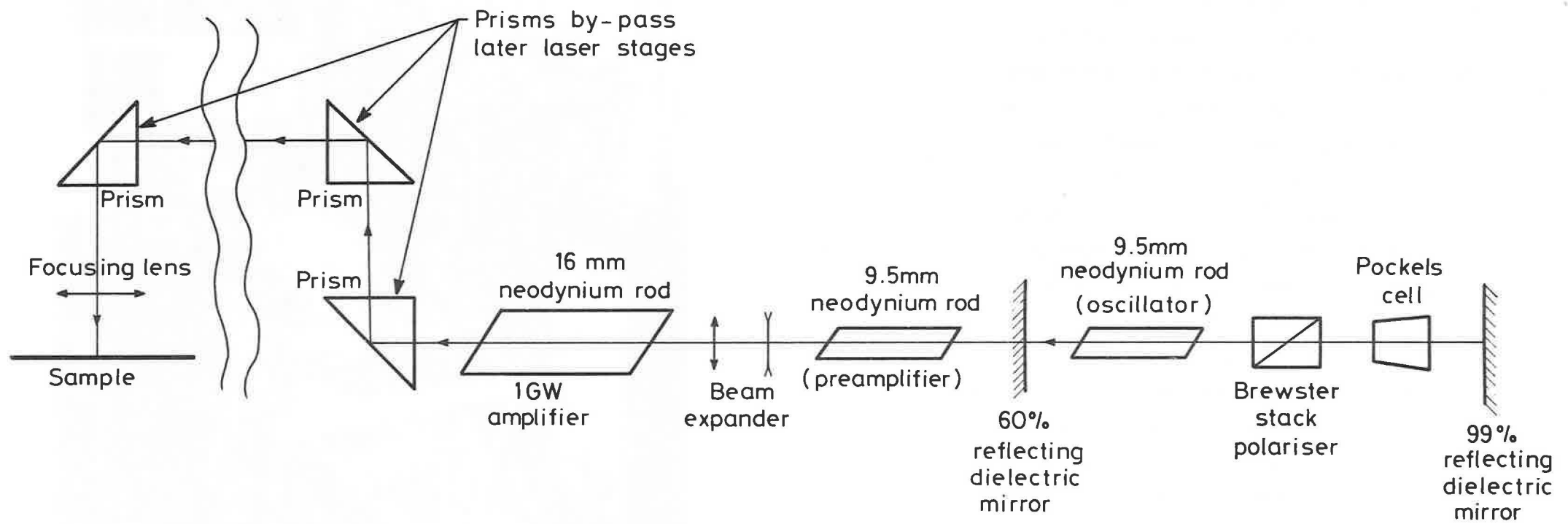
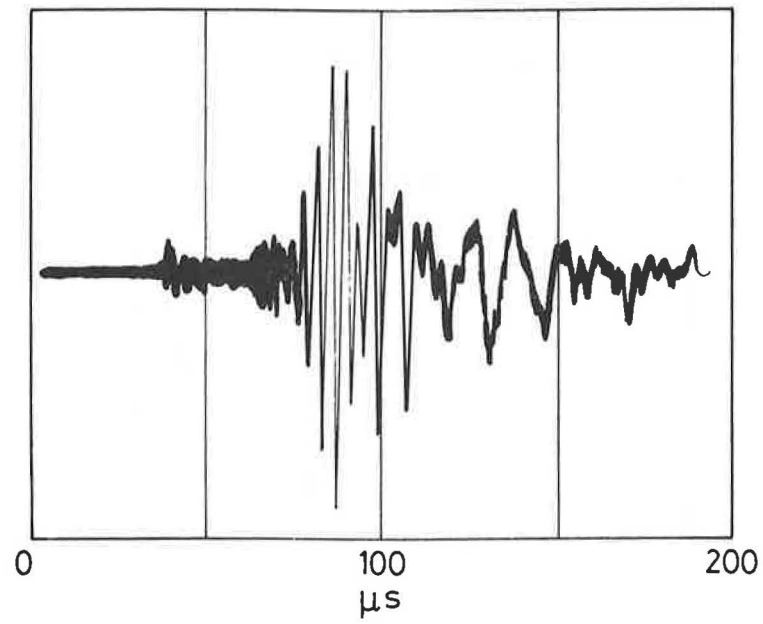
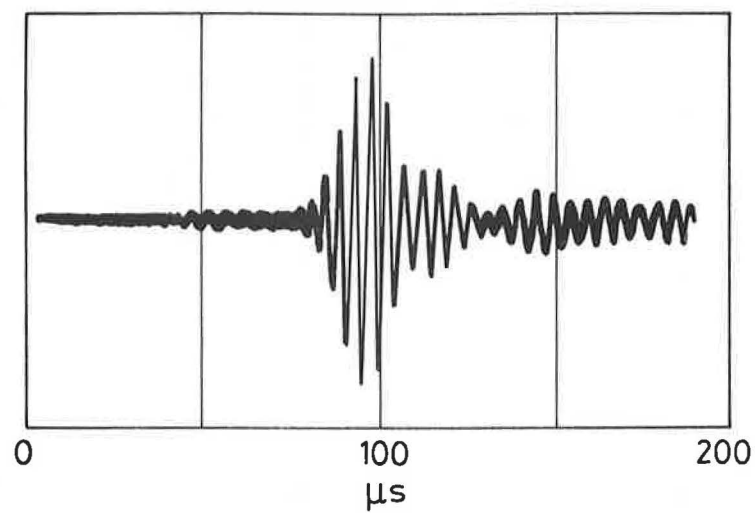


Fig.2. Schematic arrangement of laser optics



(a) No filter



(b) With 200kHz filter

Fig.3. Oscilloscope traces of flexural wave pulse

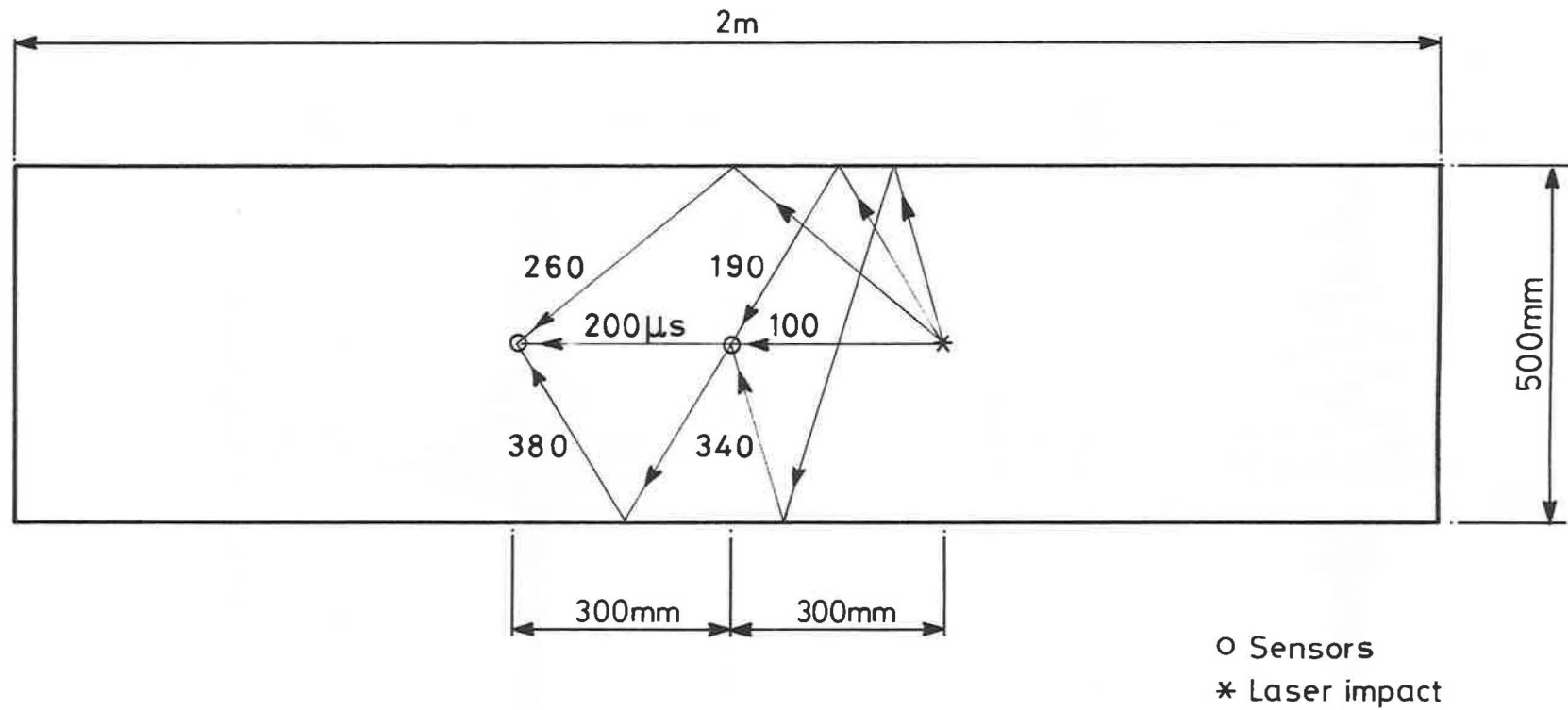


Fig.4 (a). Schematic of experimental arrangement illustrating edge reflections and observed transit times

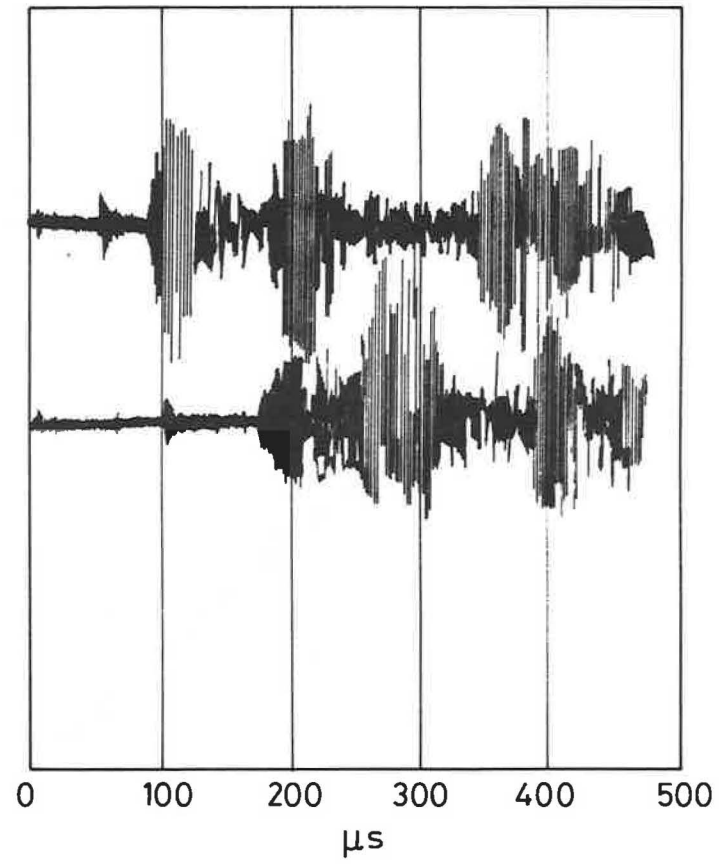


Fig. 4 (b). Oscilloscope trace obtained from experimental arrangement shown in Fig. 4 (a).

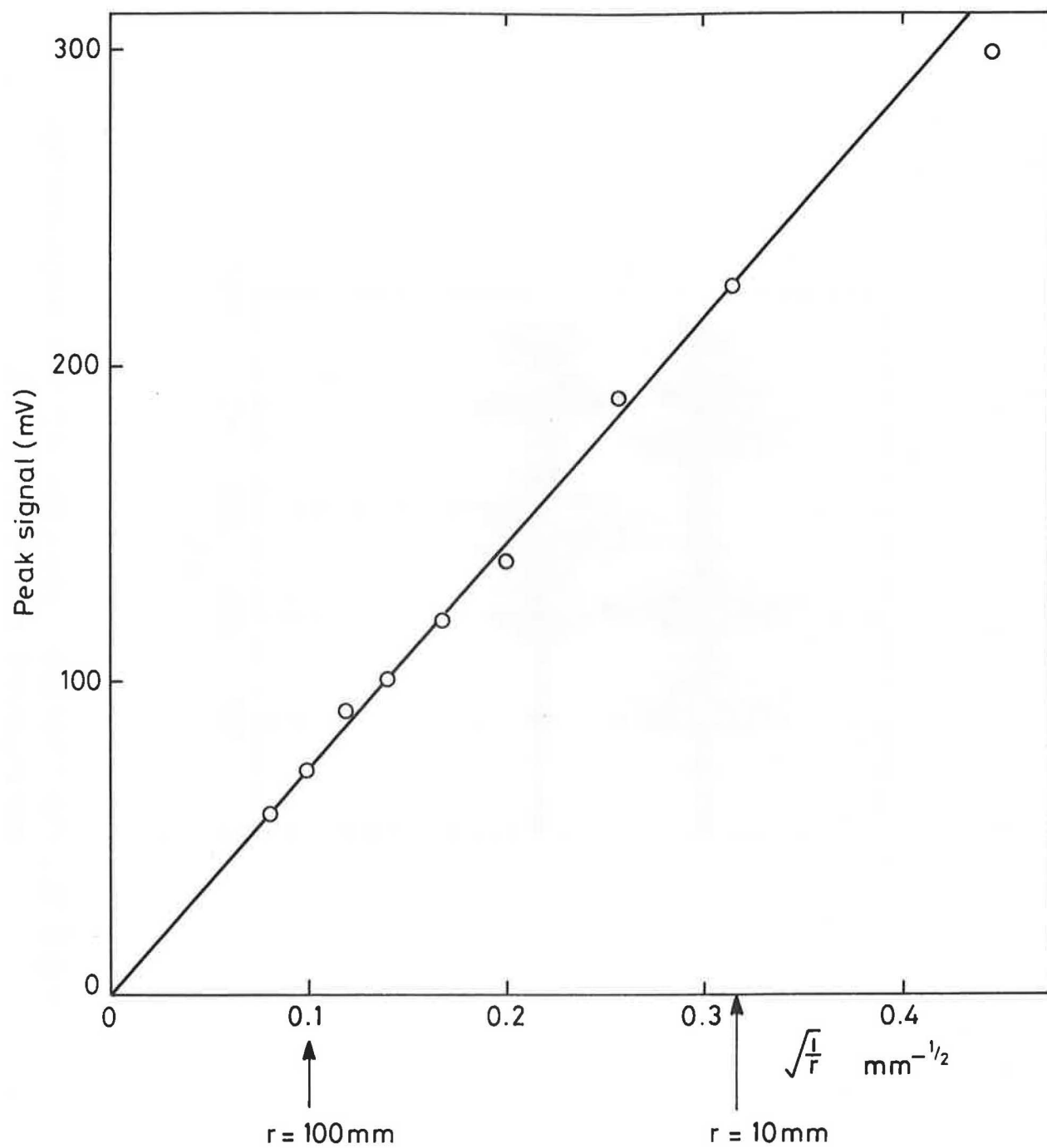


Fig. 5 . Graph showing $\sqrt{\frac{1}{r}}$ dependence of sensor response

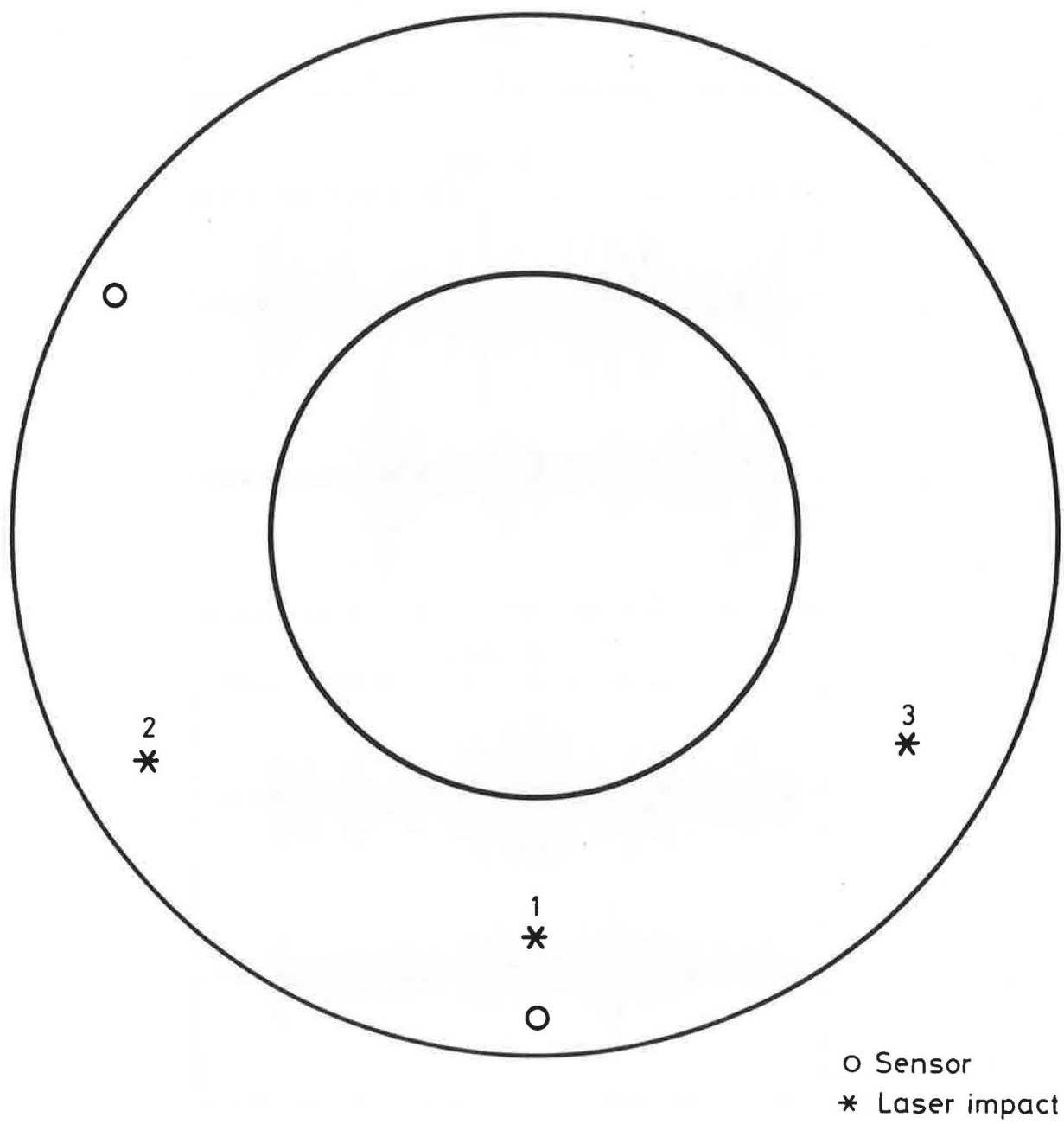
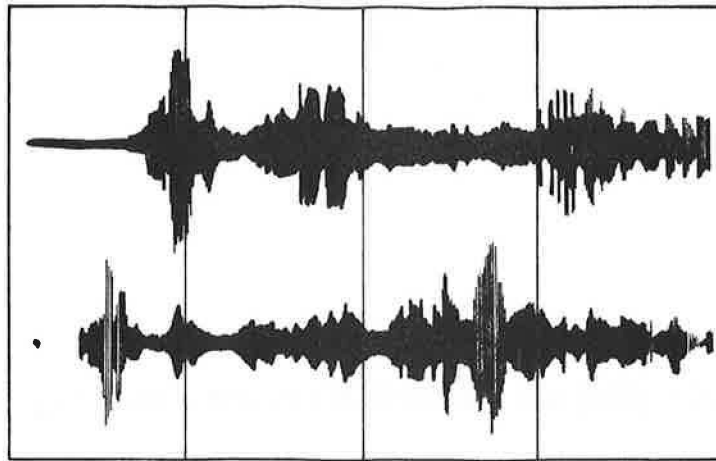
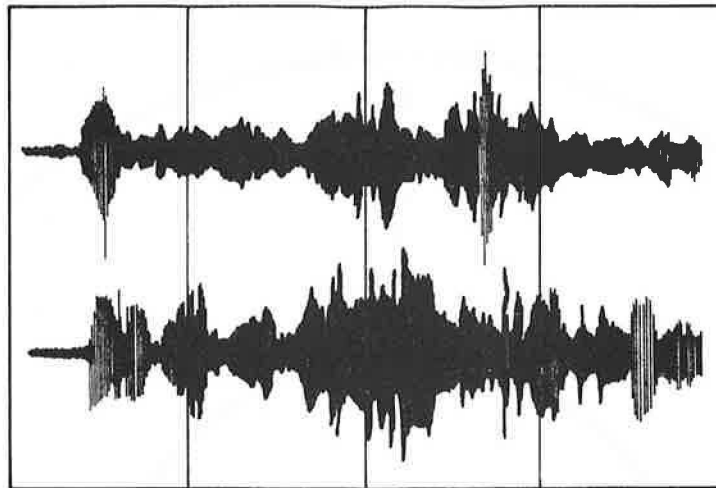


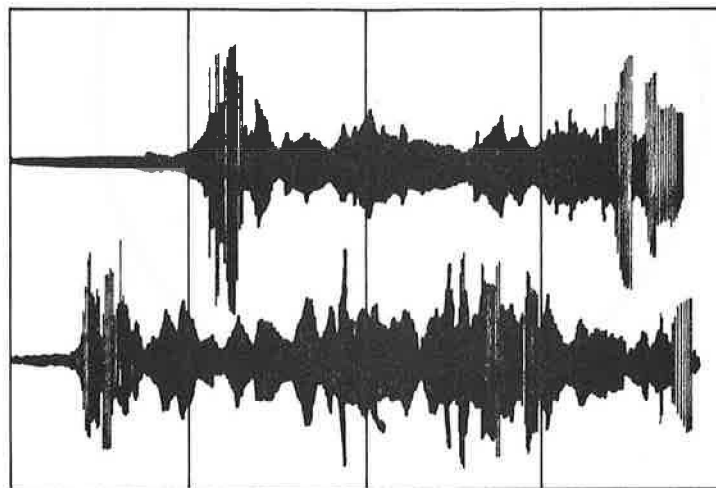
Fig.6(a). Two-sensor arrangement on half-scale annulus



Shot.1



Shot.2



Shot.3

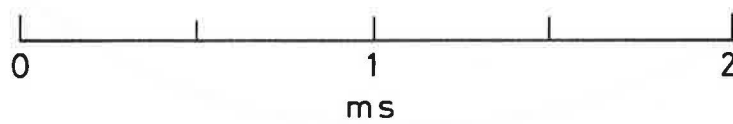
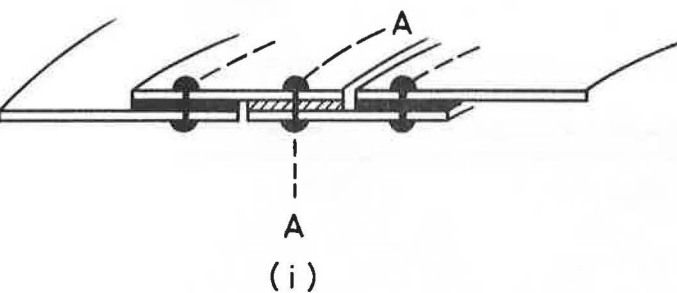
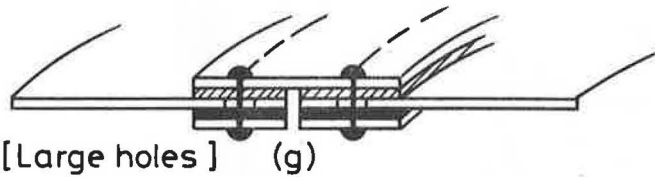
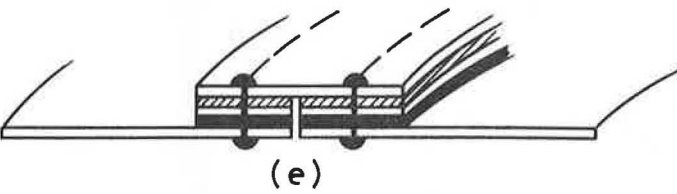
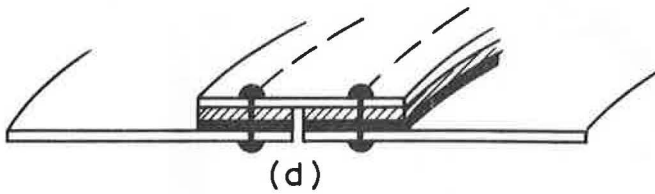
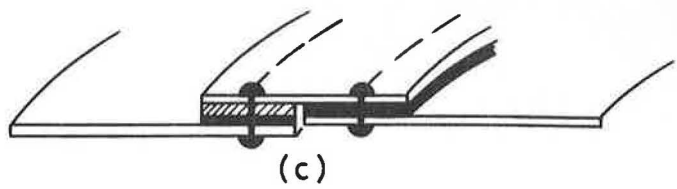
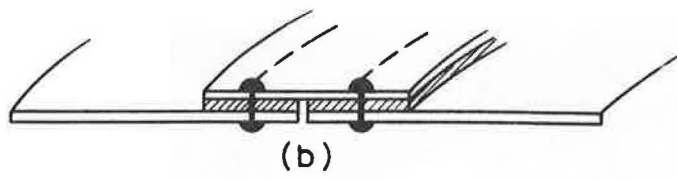
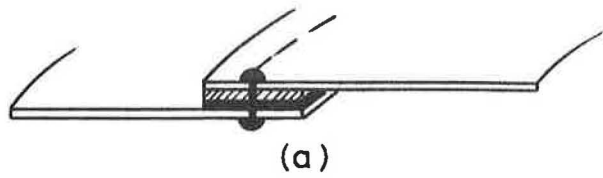
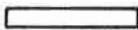


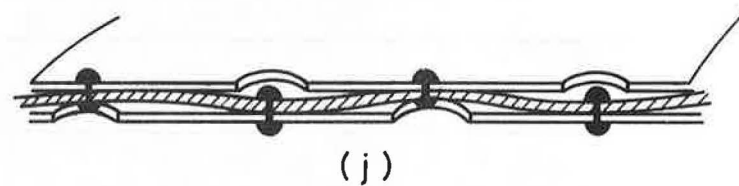
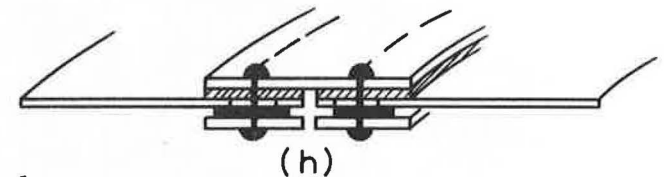
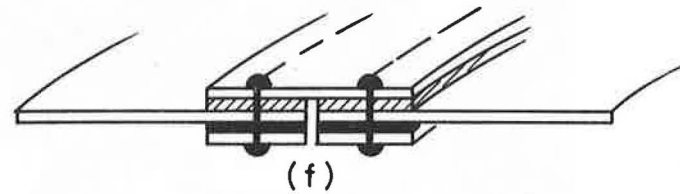


Fig.6(b). Oscilloscope traces obtained from experimental arrangement shown in Fig.6(a)



In all cases

-  is Aluminium
-  is Viton
-  is test material (maybe viton)



[Section AA on special joint (i)]

Fig.7. Various sector joints

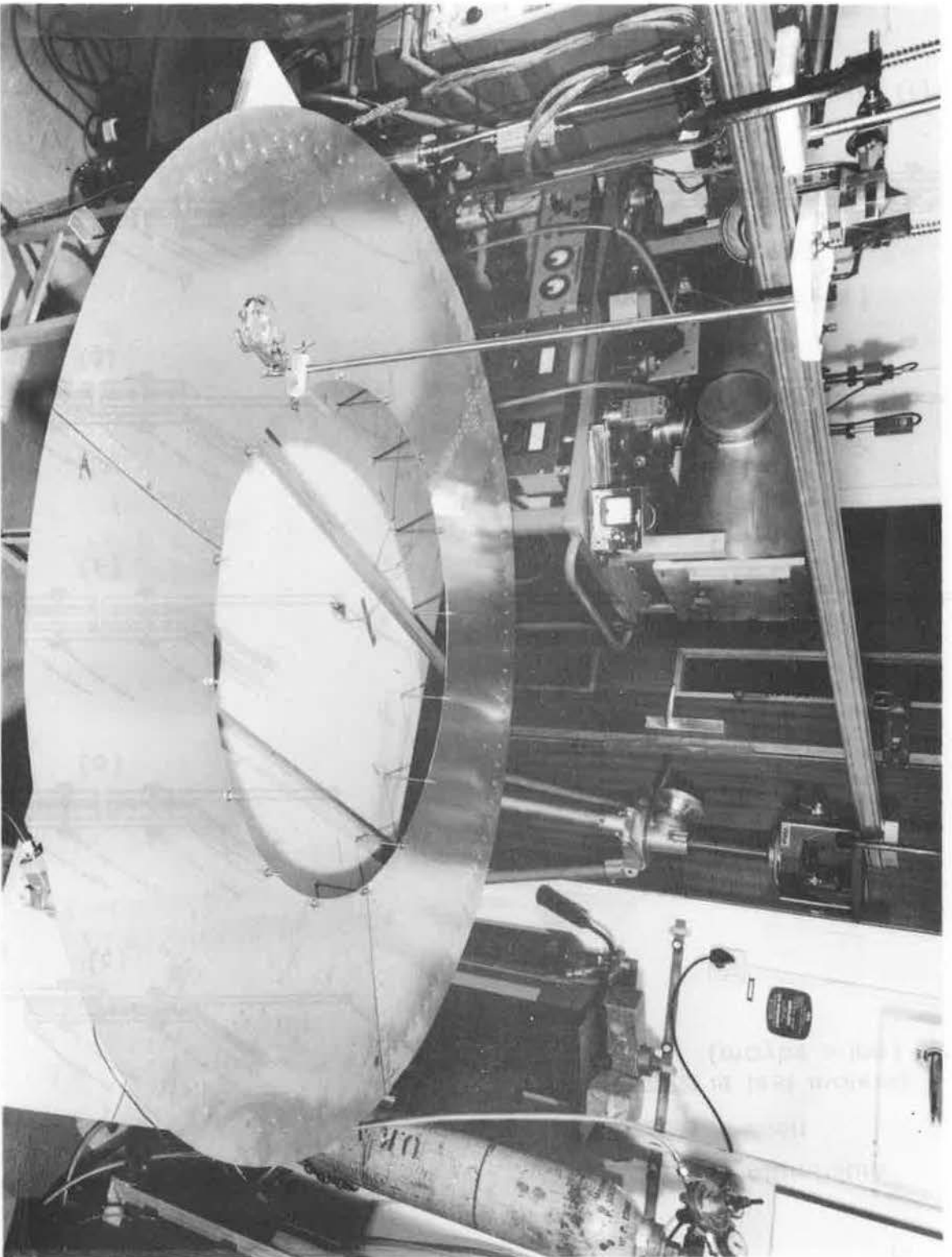


Fig. 8a Photograph of DIDSY Shield Mock-up

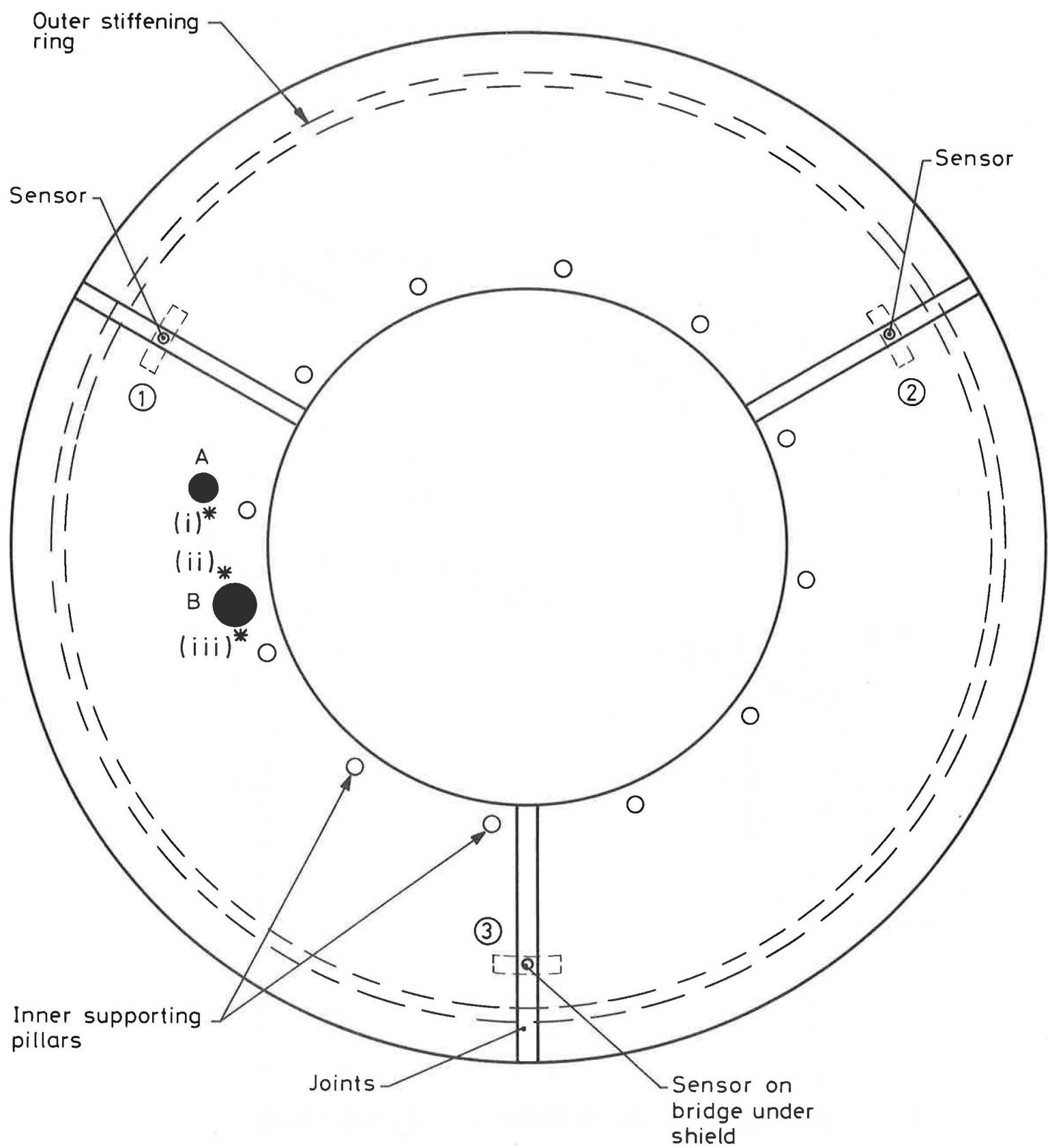


Fig. 8(b). Schematic arrangement of full-sized model of Didsy front bumper shield

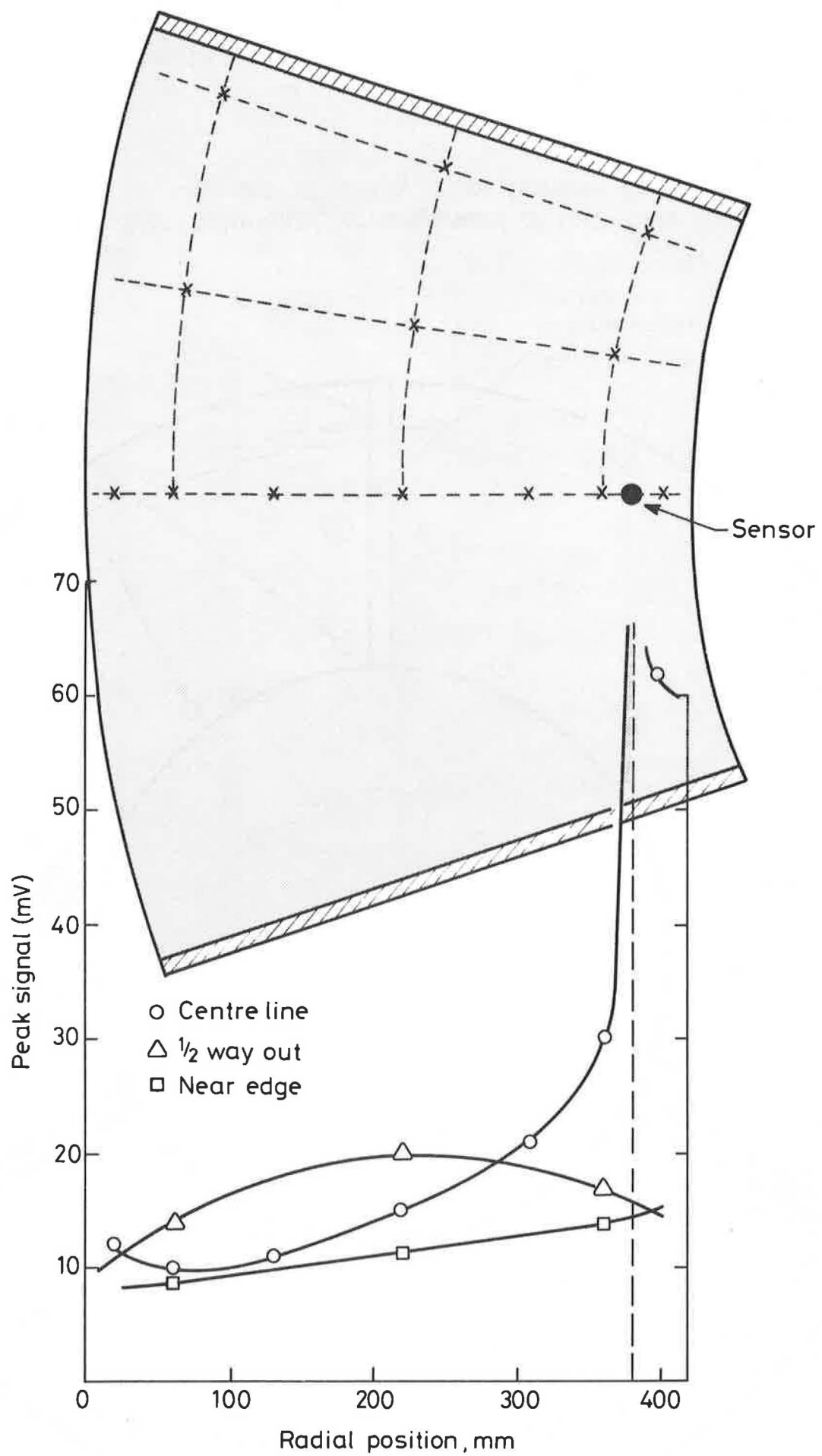


Fig. 9. Measured response over 35° Sector

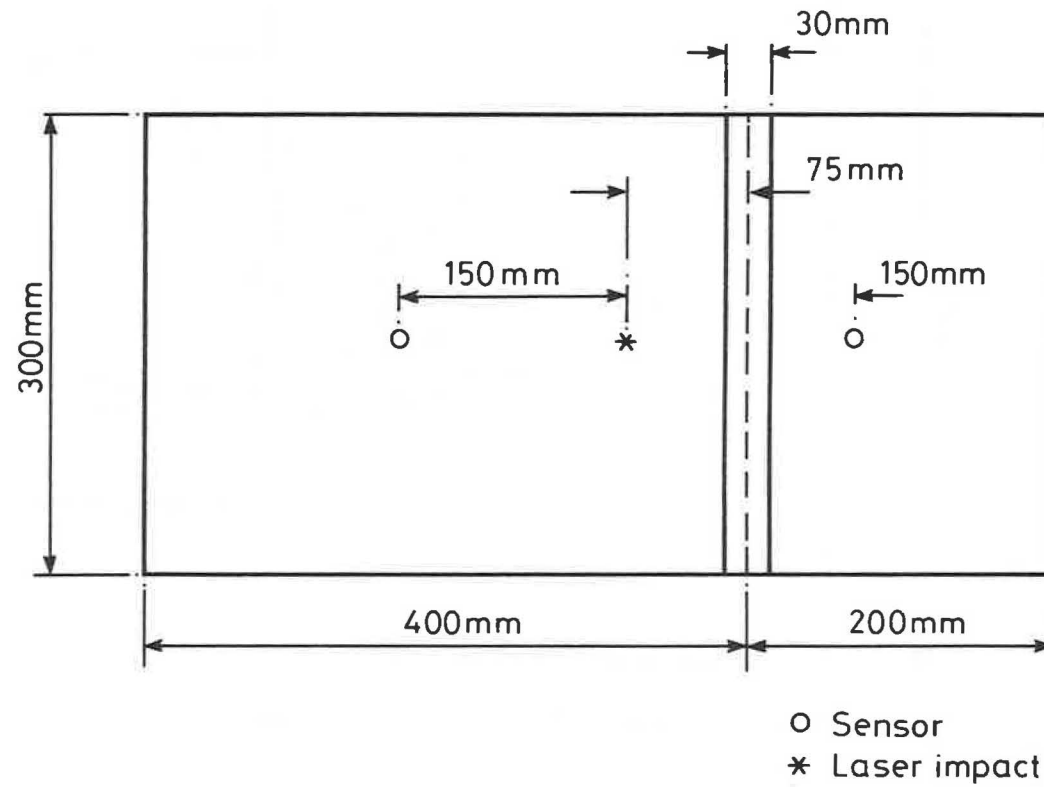


Fig.10. Schematic diagram showing experimental arrangement used to measure transmission of joints

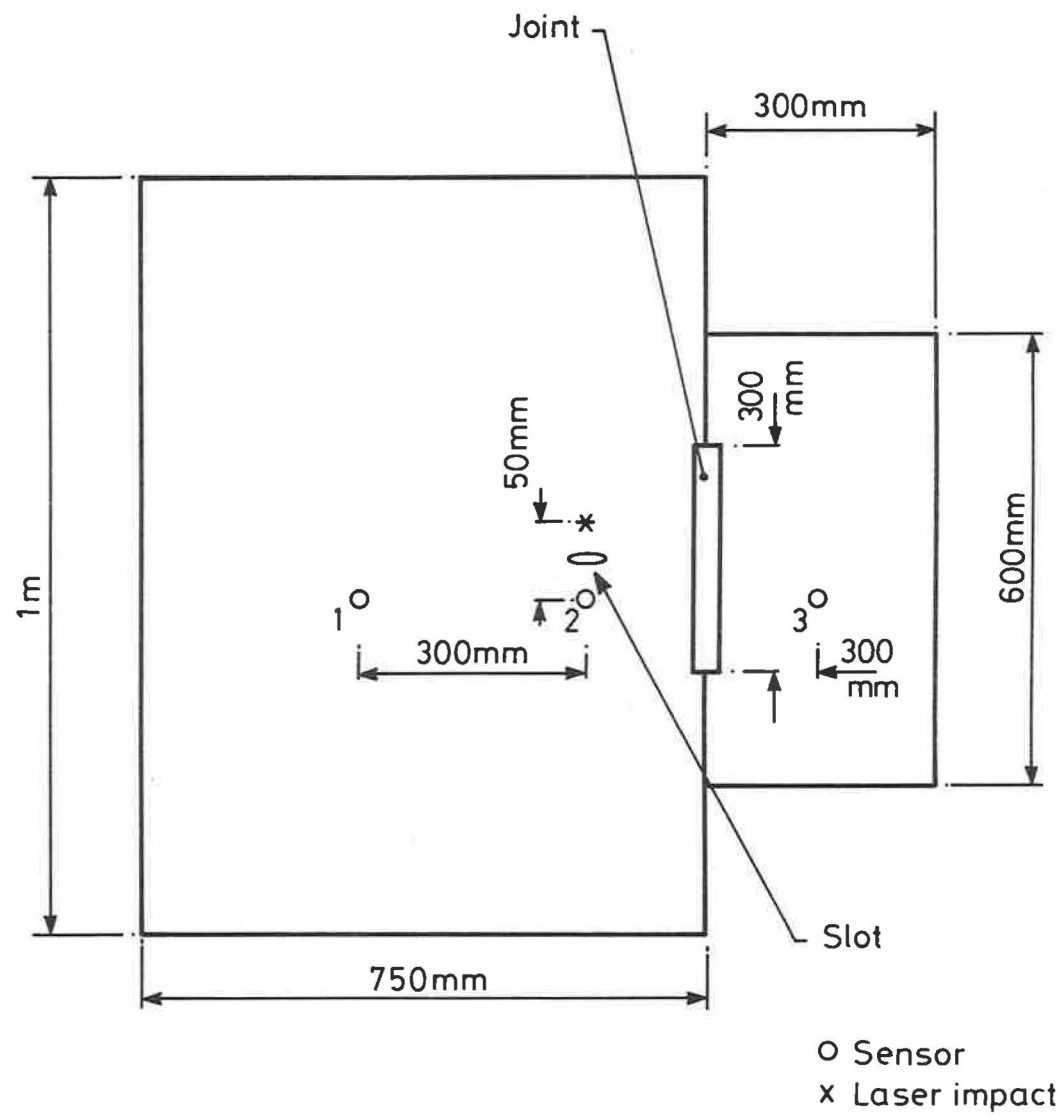


Fig.11. Experimental arrangement to measure reflectivity as well as transmission of joints

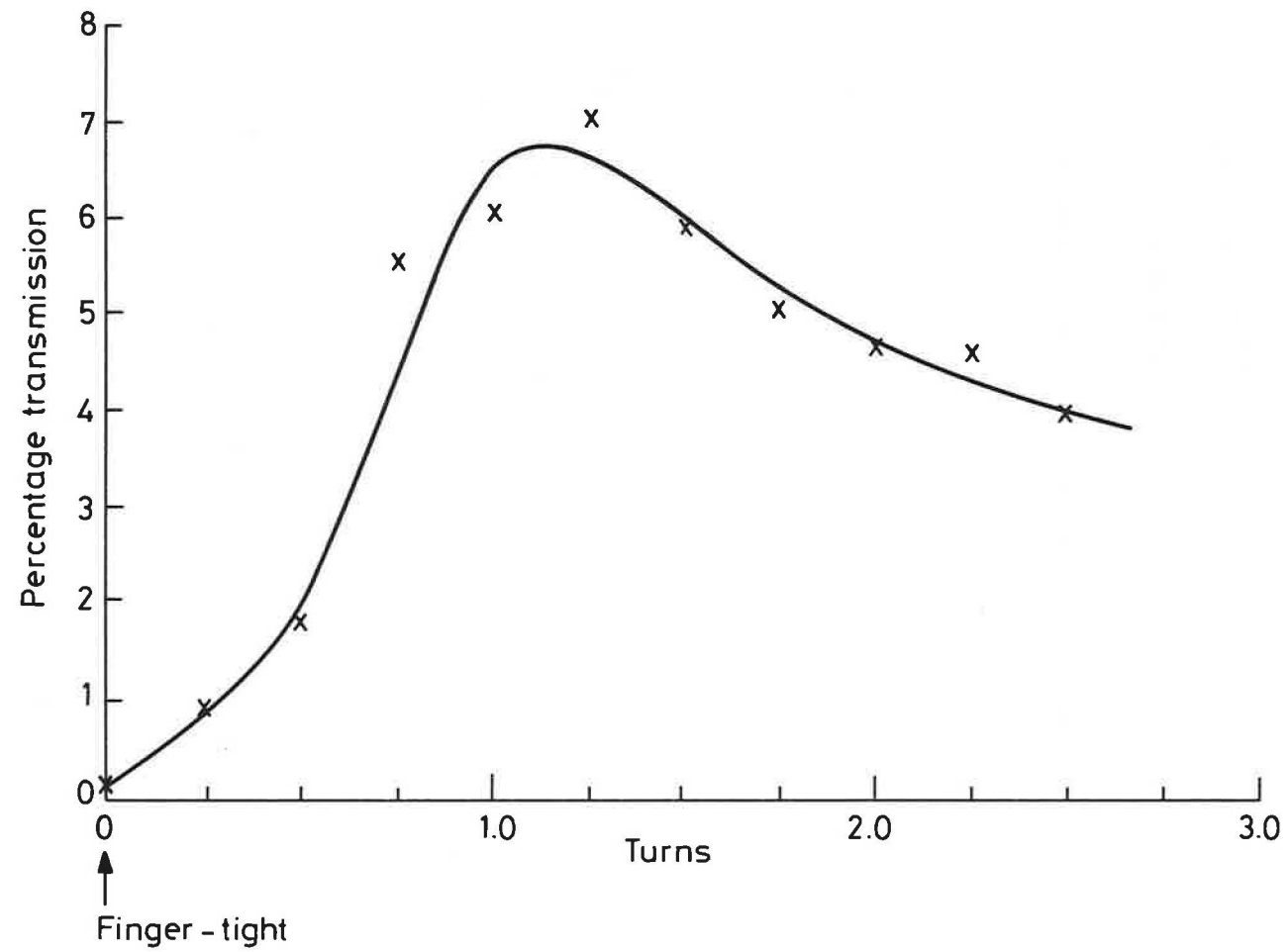


Fig.12. Effect of bolt pressure on transmission

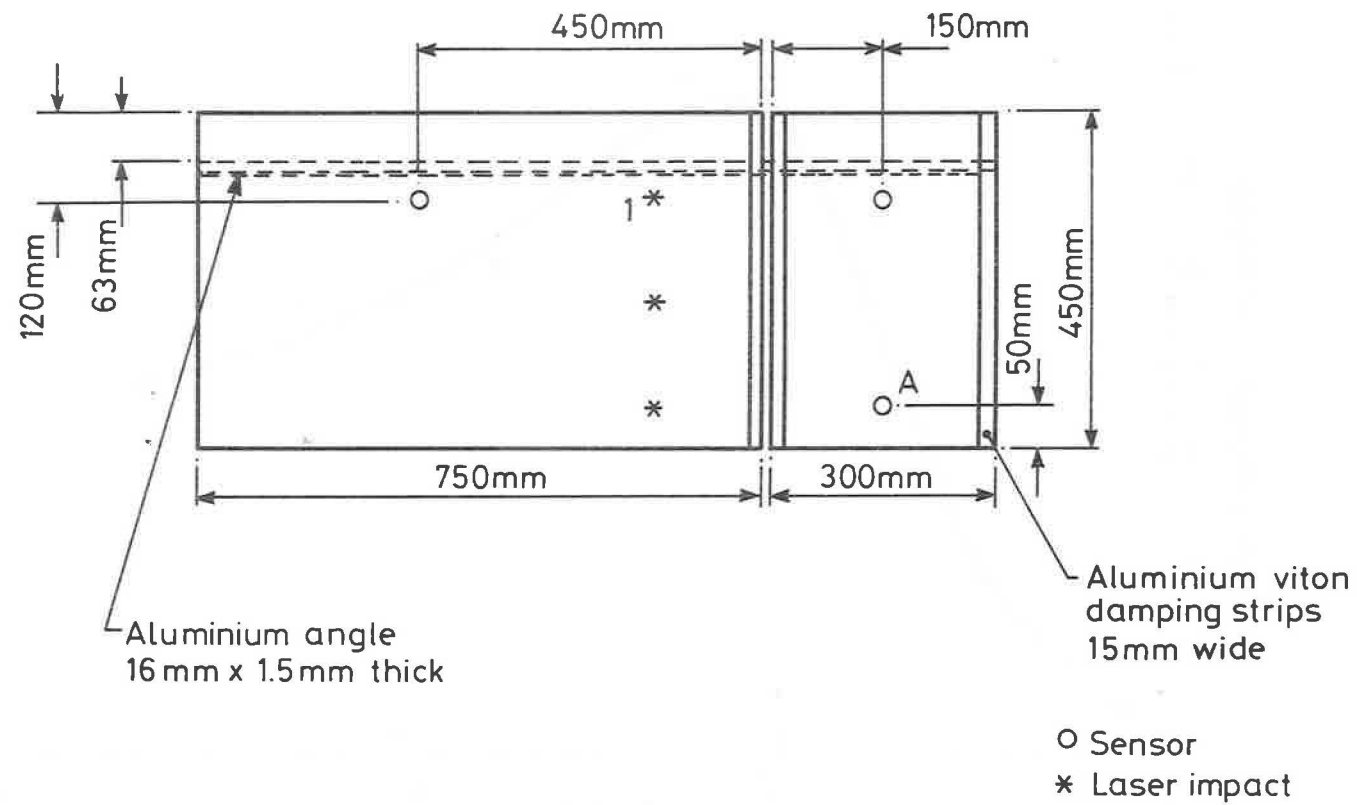


Fig.13. Experimental assembly to study effects of stiffening ring

The classical Bernoulli-Euler equation for transverse displacements w is

$$\nabla^4 w + (\rho h/D) \partial^2 w / \partial t^2 = 0 \quad (1)$$

where h is the plate thickness and $D = h^3 E / 12 (1 - \sigma^2)$. The dispersion relation for a propagating plane wave exponent $i(\underline{k} \cdot \underline{r} - \omega t)$ follows simply as

$$k^4 - (\rho h/D) \omega^2 = 0 \quad (2)$$

showing that the wave velocity and group velocity are

$$c = \omega/k = \{E/12\rho (1 - \sigma^2)\}^{1/2} h k, \quad d\omega/dk = 2c \quad (3)$$

For the GIOTTO shield take the values

$$h = 1 \text{ mm}, \quad c_p = \{E/\rho (1 - \sigma^2)\}^{1/2} = 5400 \text{ m/s} \quad (4)$$

so that the wavelength appropriate to the 200 kHz detectors is

$$\lambda = 2\pi/k = 2\pi c_p^{1/2} (h/\sqrt{12}\omega)^{1/2} = 7.0 \text{ mm} \quad (5)$$

The wave and group velocities given by (3) are 1400 m/s and 2800 m/s respectively. However, the classical theory is appropriate only for long wavelengths $\lambda \gg h$ and so perhaps not accurate for the present ratio of 7. Moreover, to describe initial transients excited in the plate an extended theory is necessary.

The Mindlin theory includes rotary inertia and shear forces, and approximates the displacements by their average \bar{w} through the plate. The plate equation (1) becomes (Ref. 1, P. 492)

$$\left(\nabla^2 - \frac{1}{\kappa^2 c_2^2} \frac{\partial^2}{\partial t^2} \right) \left(\nabla^2 - \frac{\rho h^3}{12D} \frac{\partial^2}{\partial t^2} \right) \bar{w} + \frac{\rho h}{D} \frac{\partial^2 \bar{w}}{\partial t^2} = 0 \quad (6)$$

where κ is a fitting parameter dependent on the Poisson ratio σ , given for Al as $\kappa(.335) = 0.935$ (Fig. 6.8 of Ref. 1). The dispersion relation for propagating waves follows from (6) as

$$(k^2 - \omega^2/c_2^2) (k^2 - \omega^2/c_p^2) - 12\omega^2/h^2 c_p^2 = 0 \quad (7)$$

where $c_2 = \kappa(\mu/\rho)^{1/2} = \kappa v_s$ is the speed of Rayleigh surface waves, close to the shear velocity v_s . Writing (7) as

$$c_p^2 c_2^2 \frac{k^4}{\omega^4} - \left(\frac{c_2}{c_p} + \frac{c_p}{c_2} \right) c_p c_2 \frac{k^2}{\omega^2} + 1 - \alpha = 0$$

one derives the phase and group velocities as

$$c \equiv \frac{\omega}{k} = [c_p c_2 / \{\beta + (\beta^2 - 1 + \alpha)^{1/2}\}]^{1/2} \quad (8)$$

$$\frac{d\omega}{dk} = c / [1 - (\alpha c^2 / 2 c_p c_2) (\beta^2 - 1 + \alpha)^{-1/2}]$$

where

$$\alpha = 12c_2^2/h^2\omega^2, \quad \beta = \frac{1}{2}(c_p/c_2 + c_2/c_p)$$

For the GIOTTO shield simulations, adopt the parameters given for rolled aluminium⁽²⁾

$$E = 6.8-7.1 \times 10^{10} \text{ newtons/m}, \quad \alpha = 0.355, \quad \rho = 2.70 \text{ g/cm}^3, \quad (9)$$

$$c_p = (E/\rho (1 - \sigma^2))^{1/2} = 5370-5486 \text{ m/s}, \quad v_s = (\mu/\rho)^{1/2} = 3040 \text{ m/s}$$

For a 1 mm plate at 200 kHz, (8) gives

$$\omega/k = 1297-1310 \text{ m/s}, \quad d\omega/dk = 2276-2295 \text{ m/s}, \quad \lambda = 2\pi/k = 6.5 \text{ mm} \quad (10)$$

snowing the phase velocity is down by 7% and group velocity by 18% compared with classical theory. The Mindlin theory has been found to be quantitatively very accurate compared with exact computations (Fig. 8.24, Ref. 1). For various parameters, the formulae (8) are drawn in Fig. 14, the scaling for plate thickness and frequency being combined as in α of (8). Since phase speeds ω/k for present values are about 50% of the limiting velocity κv_s , deviations from classical theory are appreciable but not large.

REFERENCES

1. Graff, K.F., "Wave Motions in Elastic Solids", Clarendon Press (1975).
2. Mason, W.P., "Acoustic Properties of Solids", Am. Inst. Phys. Handbook, Ch 3f, 3rd Ed (1972).

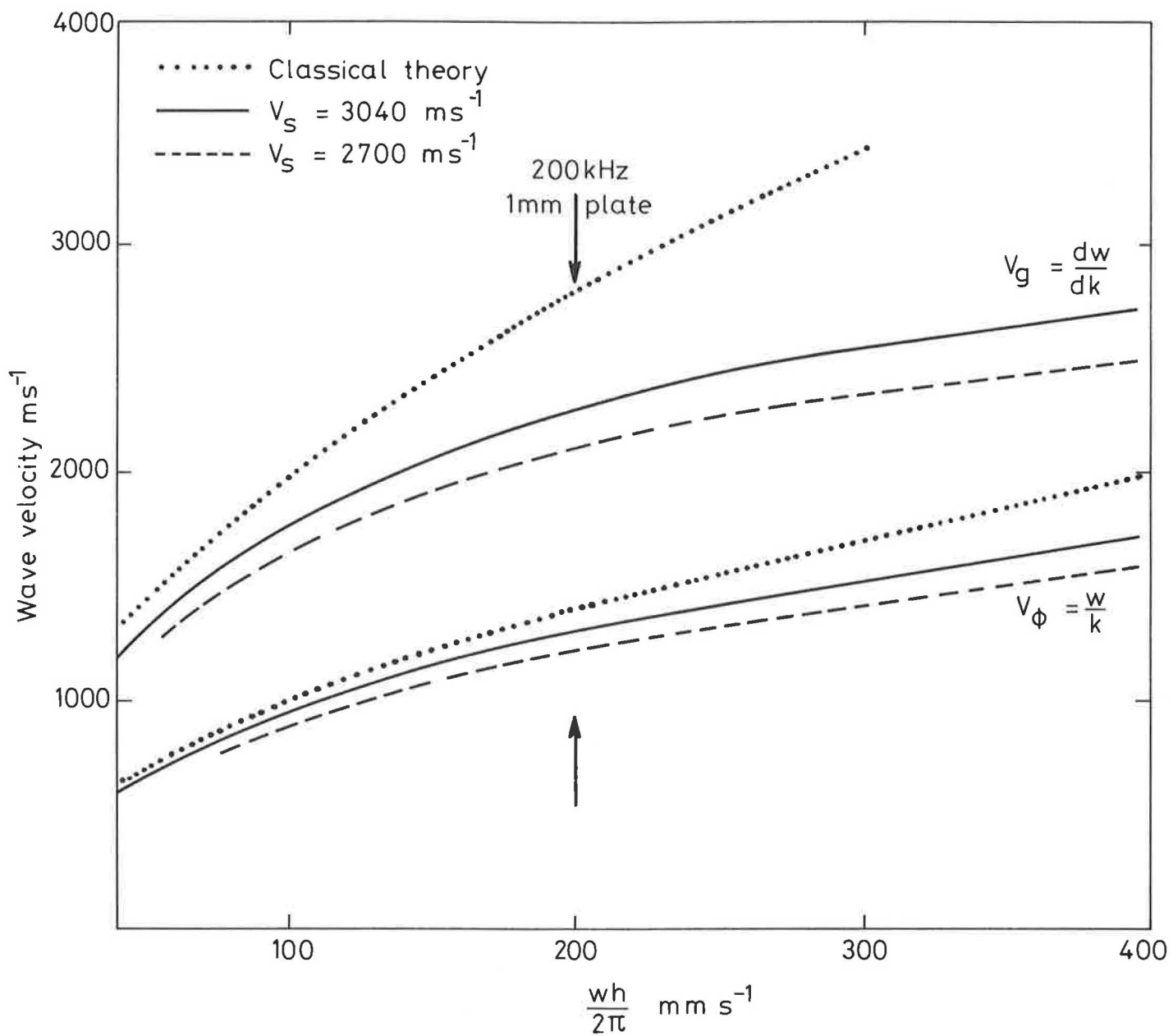


Fig. A1. Phase and group velocities of flexural waves in aluminium plates according to the Mindlin theory

